Threshold pion photoproduction on nucleons

To cite this article: D Dreschsel and L Tiator 1992 *J. Phys. G: Nucl. Part. Phys.* **18** 449

View the article online for updates and enhancements.

TOPICAL REVIEW

Threshold pion photoproduction on nucleons*

Dieter Drechsel and Lothar Tiator

Institut für Kernphysik, Universität Mainz, D-6500 Mainz, Federal Republic of Germany

Abstract. Pion photo- and electroproduction off the nucleon at threshold is reviewed in theory and experiment. In this region the leading S-wave amplitudes (E_{0+}) are predicted by low-energy theorems (LET) based on current conservation and chiral symmetry. While these predictions are in agreement with the data for charged pion production, LET cannot explain the reaction p(γ, π^0)p over the energy range of the first 10 MeV above threshold. Present calculations involving final state interactions are difficult to reconcile with the requirements of LET and suffer from a strong model dependence due to off-shell formfactors.

With the completion of the new electron accelerators with high duty factor and high intensity, new types of coincidence experiments with polarization degrees of freedom will be performed. We review the formalism for such reactions and present the multipole decomposition of the various response functions. The new experimental capabilities allow some of the most challenging problems of intermediate energy physics to be attacked, such as the puzzle of neutral pion production at threshold, the electric quadrupole amplitude in the region of the Δ resonance ('bag deformation'), the Coulomb monopole amplitude near the Roper resonance ('breathing mode'), the production of η-mesons via the N*(1535) and the production of two pions and more to test consequences of chiral symmetry and the interaction of pions at low energies.

1. Introduction

In order to explain the short-range nature of the nuclear forces, Yukawa (1935) postulated the existence of the pion. Shortly after, Kemmer (1938) formulated a *theory* of the strong interactions on the basis of invariance under rotations in isospace, taking into account the nucleon (isodoublet p, n) and the pion (isotriplet π^+, π^0, π^-). The carriers of the nuclear forces were identified experimentally much later, charged pions by Lattes *et al* (1947) and neutral pions by Panofsky *et al* (1950).

The theory of photoproduction of pions was written in the 50s. Kroll and Ruderman (1954) were the first to derive model-independent predictions in the threshold region, so-called low energy theorems (LET), by applying gauge and Lorentz invariance to the reaction $\gamma + N \rightarrow \pi + N$. The general formalism for this process was developed by Chew *et al* (1957, CGLN amplitudes). Fubini *et al* (1965) extended the earlier predictions of LET by including also the hypothesis of a partially conserved axial current (PCAC). In this way they succeeded in describing the threshold amplitude as a power series in the ratio $\mu = m_\pi/m_N$ up to terms of order

Table 1. Basic properties of π and η mesons (see Aguilar-Benitez *et al* (1990) for more details)

	i^G	j^{PC}	Mass (MeV)	Lifetime (s)	Decay modes (%)	
$\pi^\pm$	1^-	0^-	139.57	2.60×10^{-8}	$\mu\nu_\mu$	(100)
π^0	1^-	0^{-+}	134.97	8.4×10^{-17}	$\gamma\gamma$	(98.8)
					$\gamma e^+ e^-$	(1.2)
η	0^+	0^{-+}	548.8	5.5×10^{-19}	$\gamma\gamma$	(38.9)
					$3\pi^0$	(31.9)
					$\pi^+\pi^-\pi^0$	(23.6)

μ^2. Berends *et al* (1967) analysed the existing data in terms of a multipole decomposition and presented tables of the various multipole amplitudes contributing in the region up to excitation energies of 500 MeV.

The basic properties of the pion are listed in table 1. Due to electromagnetic interactions the isospin symmetry between charged and neutral pions is broken, giving rise to a mass splitting of about 5 MeV and a very dramatic decrease of the lifetime of neutral pions because of the decay $\pi^0 \rightarrow \gamma + \gamma$.

The spatial extension of the pion is an important manifestation of its internal degrees of freedom. Its form factor follows a simple monopole form,

$$F_\pi = (1 + b^2 Q^2)^{-1}.$$

Such a behaviour is predicted for $Q^2 \rightarrow \infty$ by asymptotic quantum chromodynamics, because it requires the exchange of one gluon to 'inform' the spectator quark in the pion about the scattering process. The 'root mean square' radius (RMS) is determined for small momentum transfer, its values are surprisingly close for nucleons (Simon *et al* 1981) and pions (Amendolia *et al* 1984),

$$\langle r^2 \rangle_p^{1/2} = 0.862 \pm 0.012 \text{ fm}$$

$$\langle r^2 \rangle_\pi^{1/2} = 0.657 \pm 0.012 \text{ fm}.$$

In view of this fact it seems to be a rather crude approximation to treat the pion as a point-like particle in chiral bag models or other models of the nucleon.

The original MIT model described the nucleon by three valence quarks confined to the volume of a bag by the 'pressure' of the surrounding vacuum (Chodos *et al* 1974). It was soon realized that this model does not conserve the chirality. As long as the forces at the surface do not depend on the spin of the quarks, the helicity $\sigma \cdot \hat{p}$ will change when the quarks are reflected at the surface. The chirality may be restored when the rigid surface is replaced by a pion cloud (Brown and Rho 1979, Thomas 1984), in so-called σ-models, by a 'chiral combination' of the pion and a hypothetical sigma meson. The tensor forces appearing in such chiral bag models may also lead to a deformation of the bag. Unfortunately, such an intrinsic deformation cannot be observed in the case of the nucleon due to its small spin ($\frac{1}{2}$). There are, however, observable consequences of such models for transitions from the nucleon to the Δ resonance with spin $\frac{3}{2}$ and, at least in principle, for static properties of that resonance.

We know from the theory of neutrinos that, *a priori*, chirality is only conserved for massless particles. However, QCD or QCD-inspired theories have to describe massive nucleons. Such particles may be obtained in a chirally invariant theory with

massless 'current' quarks, as non-perturbative solutions. When such massive nucleons are produced, there also appears a pion-like object at mass zero ('Goldstone boson') in such a way that overall chirality remains conserved. While the conservation of the (electric) charge may be derived as a consequence of a conserved vector current J_μ, a conserved chirality is related to a vanishing four-divergence of an axial current, $\partial^\mu J_{5\mu} = 0$. The role of chiral symmetry and the structure of pions and nucleons has recently been reviewed by Ericson and Weise (1988).

If we allow for small but finite 'current' quark masses ($m_u \simeq 5\,\text{MeV}$, $m_d \simeq 9\,\text{MeV}$, see Gasser and Leutwyler 1982), the pion obtains its finite mass and, at the same time, also the axial current is no longer conserved. Instead we obtain the PCAC relation,

$$\partial^\mu J_{5\mu} = -f_\pi m_\pi^2 \Phi^\pi$$

i.e. the axial current would be conserved if the pion was stable (pion decay constant $f_\pi \to 0$), for vanishing pion mass ($m_\pi \to 0$, as would be the case for $m_u, m_d \to 0$) and if there was no pion field ($\Phi^\pi \to 0$).

By simply counting the masses of the quark–antiquark pair in the pion and the three valence quarks in the proton, constituent quark models predict the mass ratio $\mu \simeq \frac{2}{3}$. In a model with vanishing current quark masses, on the other hand, the pion appears as a Goldstone particle leading to $\mu = 0$. The actual mass ratio $\mu \simeq \frac{1}{7}$ indicates the hybrid nature of the physical pion between Goldstone boson and q$\bar{\text{q}}$ state.

In view of the basic importance of the pion for our understanding of nucleons and nuclear forces, pion photoproduction has been and will be of considerable interest. Since this reaction is sensitive to the off-shell properties of the pion–nucleon interaction, i.e. to the short-range behaviour of the pion wavefunction, it may serve as a critical test of models of hadrons. Some of the contributions to this process are shown in figure 1, in particular the Born terms with nucleon and pion pole terms (singularity for $m_\pi \to 0$) and the seagull or Kroll–Ruderman term as well as resonance contributions in the s-channel (nucleon resonances N* and Δ) and in the t-channel (heavier mesons, e.g. ω and ρ).

Finally, the total cross section for photoabsorption on the proton is shown in figure 2. As a function of excitation energy, three main peaks are evident, corresponding to magnetic dipole (M1), electric dipole (E1) and electric quadrupole (E2). A systematic analysis of pion photoproduction experiments allows a determination of the various multipoles for the transition to each of these nucleon
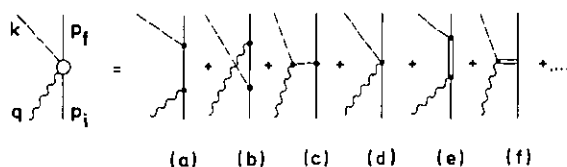

Figure 1. Diagrams contributing to pion photoproduction: (a) direct and (b) crossed nucleon pole, (c) pion pole, (d) contact term (in pseudovector coupling), (e) isobar excitation, (f) exchange of heavier mesons.
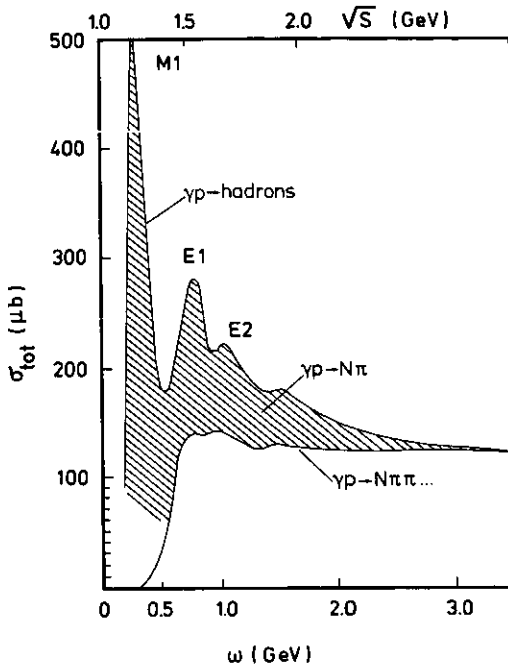
Figure 2. The total photoabsorption cross section for the proton and its decomposition into exclusive channels, as a function of the photon energy (see Gross 1986 for details).

resonances, thereby providing a large set of phenomenological quantities to be compared with the theoretical models. Of particular interest are:

(i) the distribution of magnetism (M1) in the first resonance region of the $\Delta(1232)$ or P_{33} resonance. There is also a small ($\approx 1\%$) E2 admixture in this region as a consequence of the bag deformation,

(ii) the splitting of the E1 strength in the second resonance region into two resonances, $N(1520)$ or D_{13} and $N(1535)$ or S_{11}. The two states are predicted to behave quite differently at large momentum transfer. Moreover, the S_{11} state shows a strange and as yet unexplained decay into η mesons (50%),

(iii) the concentration of the E2 strength in the third resonance region related to a deformation or rotation of the nucleon,

(iv) the search for the breathing mode of the nucleon (Coulomb monopole strength, C0) in the region of the Roper resonance $N(1440)$. Obviously, this mode is strongly influenced by the bag pressure and the compressibility of hadronic matter. Since this level has only a small M1 strength, it gives only a small contribution for real photons as in figure 2.

In view of the low energy theorem (LET), threshold pion production on the nucleon was considered to be well understood until a few years ago. In fact, low energy pion production was used to study the structure of nuclei and possible medium modifications of the elementary photoproduction operator. Therefore it came as a big surprise when a reanalysis of the Saclay data (Mazzucato *et al* 1986) showed that the experimental threshold amplitude E_{0+} for the reaction $\gamma + p \rightarrow \pi^0 + p$ was smaller than the prediction of LET by about a factor of five. The more detailed Mainz data (Beck *et al* 1990) essentially confirm that strength is missing in the threshold region and even add to the puzzle by showing, in a somewhat model-dependent analysis, a rapid fluctuation of this amplitude over the first few MeV above threshold.

In the following section 2 we will outline the formalism for pion photo- and electroproduction, including polarization degrees of freedom. The existing experimental data in the threshold region will be presented in section 3, and confronted with the predictions of LET in section 4. Next we will briefly review the existing models of pions and nucleons (section 5) and discuss higher order corrections to LET as derived from such models (section 6). We conclude with a short summary of the present status of threshold pion photoproduction in section 7.

2. Formalism

2.1. Kinematics

Since the electromagnetic interaction is governed by the fine structure constant $\alpha = e^2/4\pi$, the one-photon exchange approximation (see figure 3) has an accuracy of about 1% for electron scattering from the proton. In this limit, the electron tests the hadronic currents at a well defined energy and momentum transfer. The 4-momentum of the exchanged photon, $q = (\omega, q) = k_i - k_f$, is fixed by the 4-momenta of the incident and outgoing electrons, $k_i = (\varepsilon_i, k_i)$ and $k_f = (\varepsilon_f, k_f)$, respectively.

The independent variation of q and ω in an electron scattering experiment allows the spatial distribution of the physical phenomena under investigation to be explored. In this context it is common to use the positive quantity $Q^2 = -q^2$ to describe form factors and structure functions. Obviously, Q^2 vanishes for real photons.

The kinematics of the nucleon target is described by the 4-vector $P_i = (E_i, P_i)$ in the initial state. In general we will refer to a typical two-arm experiment, i.e. an emitted pion with $k = (\omega_\pi, k)$ is observed in coincidence with the scattered electron, and the recoiling nucleon carries the momentum $P_f = (E_f, P_f)$. The inclusive (one-arm) process may then be obtained by integrating and summing over the hadronic momenta in all possible decay channels.

Due to momentum conservation there are three independent momenta at the hadronic vertex, e.g. q, P_i and k. Since both the target system and the detected decay products are on-shell, $P_{i,f}^2 = m_{i,f}^2$ and $k^2 = m_\pi^2$, there are three independent scalars, which may be chosen to be the momentum transfer and two of the three
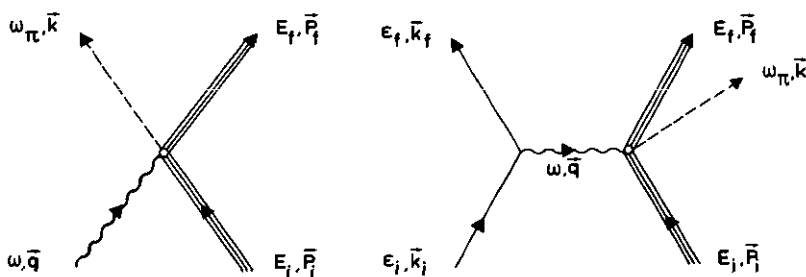

Figure 3. The kinematic variables for: (left) pion photoproduction and (right) a two-arm electroproduction experiment in the one-photon exchange approximation. The spins of the particles are $s_{i,f}$ and $S_{i,f}$ for the initial and final states of electrons and nucleons, respectively. The photon has the polarization vector $\varepsilon^\mu(\lambda)$.

Mandelstam variables,

$$\{Q^2, s = W^2 = (P_i + q)^2, t = (q - k)^2, u = (P_i - k)^2\}.$$

The threshold laboratory energy ω_L for the production of a particle with mass m_π is obtained by evaluating the variable s in the laboratory and centre-of-mass (CM) frames

$$\omega_L^{th} = \frac{(m_f + m_\pi)^2 - m_i^2 + Q^2}{2m_i}. \tag{1}$$

Similarly, a resonance in the hadronic final state at a mass W occurs for

$$\omega_L^{res} = \frac{W^2 - m_i^2 + Q^2}{2m_i}. \tag{2}$$

2.2. Transition current and invariant amplitudes

Since the current operator has to reflect the negative parity of the pion, the general structure of the transition current between initial and final nucleon states is given by (de Baenst 1970)

$$\hat{J}_\mu = (A\tilde{\gamma}_\mu + B\tilde{P}_\mu + Ck_\mu)\gamma_5 + (D\tilde{\gamma}_\mu + E\tilde{P}_\mu + Fk_\mu)\gamma_5\slashed{q} \tag{3}$$

where $P = \frac{1}{2}(P_i + P_f)$ and all 4-vectors are explicitly gauge invariant, $\tilde{\gamma}_\mu = \gamma_\mu - (\gamma \cdot q/q^2)q_\mu$.

Evaluated between Dirac spinors, an equivalent form may be given in terms of the spin operator and of the unit vectors $\hat{k} = \hat{k}_{CM}$ and $\hat{q} = \hat{q}_{CM}$ of the independent momenta in the CM frame, which defines the CGLN amplitudes F_i (Chew *et al* 1957)

$$J = \frac{4\pi W}{m} (i\tilde{\sigma}F_1 + (\sigma \cdot \hat{k})(\sigma \times \hat{q})F_2 + i\tilde{k}(\sigma \cdot \hat{q})F_3$$

$$+ i\tilde{k}(\sigma \cdot \hat{k})F_4 + i\hat{q}(\sigma \cdot \hat{q})F_5 + i\hat{q}(\sigma \cdot \hat{k})F_6) \tag{4}$$

$$\rho = \frac{4\pi W}{m} (i(\sigma \cdot \hat{k})F_7 + i(\sigma \cdot \hat{q})F_8) = \frac{q \cdot J}{\omega} \tag{5}$$

with $\tilde{\sigma} = \sigma - (\sigma \cdot \hat{q})\hat{q}$ etc. In order to be consistent with previous notations for the CGLN amplitudes and their multipole decomposition, we have introduced a factor $4\pi W/m$. In this way the current can be calculated directly from Feynman diagrams in the notation of Bjorken and Drell (1964). The structure functions F_1, F_2, F_3 and F_4 describes the transverse current while the longitudinal component is given by F_5 and F_6. These structure functions depend on three variables, e.g. the square of the 4-momentum transfer Q^2 and on two of the Mandelstam variables (s and t or, alternatively, ω_L and Θ_π^{CM}). Due to the strong interaction in the πN system, they have complex values. Therefore, there are six absolute values and five relative

Table 2. Thresholds ω_L^{th} for light meson production in MeV.

	π^+	π^-	π^0	η
p	151.43	—	144.68	709.3
n	—	148.45	144.67	709.1

phases that have to be determined in each kinematical situation. Since the number of independent structure functions is connected with the spin degrees of freedom of the interacting particles, a complete determination of the structure functions requires polarization experiments. Instead of the CGLN amplitudes one often uses helicity amplitudes (Amaldi *et al* 1979, Foster and Hughes 1983, Burkert 1986) defined by transitions between eigenstates of the helicities of nucleon and photon.

Gauge invariance implies that the charge can be replaced by the longitudinal current or vice versa. This means that the coincidence cross section can be expressed by the six structure functions describing the transition current in the case of electroproduction, while there are only four invariants for photoproduction (Amaldi *et al* 1979, Drechsel and Giannini 1989).

2.3. Multipole decomposition

Since the electromagnetic interaction is treated to first order in the coupling constant, the complexity of the structure functions is completely due to the pion–nucleon interaction (Fermi–Watson theorem). Therefore, each partial wave component (α) of the structure functions may be written in the form (Watson 1954)

$$F_i^\alpha = e^{i\delta_\alpha} R_i^\alpha \tag{6}$$

where R_i^α is a real function of the kinematical values and $\delta_\alpha = \delta_\alpha(\omega_\pi^{CM})$ is the phase shift for elastic πN scattering in that particular channel $\alpha = \{lJI\}$. Including spin–orbit forces and isospin degrees of freedom the pion–nucleon system is described by $X_{2I+1, 2J+1}$, where $X = S, P, D, \ldots$ denotes the orbital angular momentum $l = 0, 1, 2, \ldots$. The total isospin of the system I can be $\frac{1}{2}$ or $\frac{3}{2}$, and $J = |l \pm \frac{1}{2}|$ is the total spin. The phase shifts for the more important pion–nucleon states are shown in figure 4. We note in particular the perfect resonance shape of the P_{33}
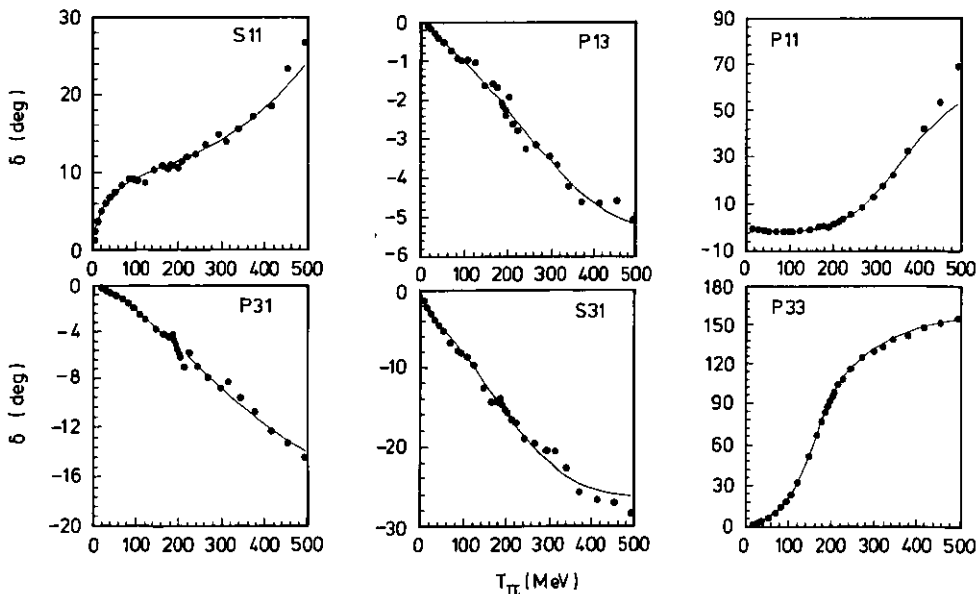

Figure 4. Pion–nucleon phaseshifts δ as a function of kinetic energy T_π^L in some selected channels $X_{2I+1, 2J+1}$ (figure from Nozawa *et al* (1990)).

phase shift corresponding to the $\Delta(1232)$ resonance of the nucleon ($\delta = 90°$ at $T_\pi^L \simeq 180\,\text{MeV}$). The steep rise of the P_{11} phase shift for $T_\pi^L \to 500\,\text{MeV}$ is an indication of the Roper resonance N(1440). In addition there is some background scattering due to interactions in the S_{11} and S_{31} states. All other phase shifts are very small for kinetic energies $T_\pi^L \le 500\,\text{MeV}$. Finally we note that the phase shifts become complex above the two-pion threshold, $\delta_\alpha \to \delta_\alpha + i\eta_\alpha$.

The analysis requires an angular momentum decomposition in both initial and final states. In the *initial state* the photon carries spin 1 and has orbital momentum $\bar{l}$ relative to the target nucleon. Its wavefunctions can be characterized by vector spherical harmonics,

$$Y_{\bar{l}LM} = \sum_v C(1\lambda, \bar{l}v \,|LM)\hat{e}_\lambda Y_{\bar{l}v}(\hat{r})$$

the transverse polarizations $\lambda = \pm 1$ leading to electric and magnetic multipole transitions EL and ML, the longitudinal polarization $\lambda = 0$ leading to longitudinal or Coulomb transitions, CL.

The *final state* is described by an orbital momentum l of the pion relative to the recoiling nucleon, with parity $(-1)^{l+1}$ due to the intrinsic parity of the pion. The total spin of the final state, J, has to equal the total spin of the initial state,

$$J = |l \pm \tfrac{1}{2}| = |L \pm \tfrac{1}{2}|.$$

Using parity arguments, we find for

CL, EL: $(-1)^L = (-1)^{l+1} \to |L - l| = 1$

ML: $(-1)^{L+1} = (-1)^{l+1} \to L = l.$

As an example, the lowest electromagnetic excitation modes and the corresponding states of the pion–nucleon system are given in table 3. The first two columns denote the familiar electromagnetic multipoles. In the next two columns we find the spin and angular momentum of the πN-system. As an example, the $\Delta(1232)$ resonance with $J = \tfrac{3}{2}$ and $l = 1$ (i.e. positive parity, including the intrinsic parity of the pion!) can be excited by both M1 and E2/C2 radiation. Its multipoles are denoted by M_{1+} and E_{1+}/L_{1+}, respectively. Here the first index characterizes the orbital momentum, $l = 1$, and the second one, the '+' sign, reminds us that spin and orbital momentum of the nucleon are parallel ($J = l + \tfrac{1}{2}$). The excitation of the Roper, N(1440) with $J = \tfrac{1}{2}$, $l = 1$ (the 'breathing mode' of the nucleon) can be reached by C0 and M1

Table 3. Amplitudes for pion electroproduction (for notation see text).

L	Electromagnetic multipole	πN system J	l	Pion production multipole
0	C0	1/2	1	L_{1-}
1	E1/C1	1/2	0	E_{0+}/L_{0+}
		3/2	2	E_{2-}/L_{2-}
	M1	1/2	1	M_{1-}
		3/2	1	M_{1+}
2	E2/C2	3/2	1	E_{1+}/L_{1+}
		5/2	3	E_{3-}/L_{3-}
	M2	3/2	2	M_{2-}
		5/2	2	M_{2+}

radiation, the multipoles L_{1-} and M_{1-}, respectively ($J = l - \frac{1}{2}$). The longitudinal multipoles are related to 'scalar' multipoles by $\omega S_{l\pm} = |q| L_{l\pm}$.

From the nature of the partial waves it is apparent that only S waves remain near threshold; for $k_{CM} \rightarrow 0$, only the multipoles E_{0+} and L_{0+} contribute. In the Siegert limit $q_{CM} \rightarrow 0$ (occasionally called 'pseudothreshold'), the transverse electric and longitudinal multipoles are related by gauge invariance,

$$E_{l\pm} \rightarrow \pm \tfrac{1}{2}(2J + 1)L_{l\pm} \qquad \text{('pseudothreshold')}. \tag{7}$$

The structure functions can be decomposed into a multipole series (Amaldi *et al* 1979) in terms of derivatives of the Legendre polynomials P_l

$$F_1 = \sum_{l \geqslant 0} \{(lM_{l+} + E_{l+})P'_{l+1} + [(l + 1)M_{l-} + E_{l-}]P'_{l-1}\}$$

$$F_2 = \sum_{l \geqslant 1} [(l + 1)M_{l+} + lM_{l-}]P'_l$$

$$F_3 = \sum_{l \geqslant 1} [(E_{l+} - M_{l+})P''_{l+1} + (E_{l-} + M_{l-})P''_{l-1}]$$

$$F_4 = \sum_{l \geqslant 2} (M_{l+} - E_{l+} - M_{l-} - E_{l-})P''_l \tag{8}$$

$$F_5 = \sum_{l \geqslant 0} [(l + 1)L_{l+}P'_{l+1} - lL_{l-}P'_{l-1}]$$

$$F_6 = \sum_{l \geqslant 1} [lL_{l-} - (l + 1)L_{l+}]P'_l.$$

The Legendre polynomials are functions of the polar angle of the pion in the CM frame, $\Theta = \Theta_\pi^{CM}$. The electric and magnetic multipoles, $E_{l\pm}$ and $M_{l\pm}$ respectively, and the longitudinal multipoles $L_{l\pm}$ depend on both energy W and momentum transfer Q^2. In the region up to about 500 MeV, the leading multipoles have been tabulated by Berends *et al* (1967).

2.4. Isospin amplitudes

The initial state is characterized by the target nucleon with isospin $\frac{1}{2}$ coupling to the electromagnetic current with the isospin structure $\sim \frac{1}{2}(f^s + f^v \tau_0)$, i.e. containing an isoscalar and an isovector component. In the final state, the pion is an isovector particle ($\boldsymbol{\Phi}$). Assuming isospin conservation in the hadronic system, the interaction in isospace has to be $\sim \boldsymbol{\tau} \cdot \boldsymbol{\Phi}$. The Pauli matrices appearing in the interaction of the nucleon with the photon and pion may be arranged in the overall matrix element in a symmetrical form

$$A = \tfrac{1}{2}A^{(-)}[\tau_\alpha, \tau_0] + A^{(+)}\delta_{\alpha 0} + A^{(0)}\tau_\alpha \tag{9}$$

where the first two terms are the commutator and anticommutator of τ_α with the isovector electromagnetic current while the last term corresponds to the isoscalar current. In terms of the three isospin amplitudes, the four physical amplitudes are obtained as

$$A(\gamma p \rightarrow n\pi^+) = \sqrt{2}(A^{(-)} + A^{(0)}) \qquad A(\gamma n \rightarrow p\pi^-) = -\sqrt{2}(A^{(-)} - A^{(0)})$$

$$A(\gamma p \rightarrow p\pi^0) = A^{(+)} + A^{(0)} \qquad\qquad A(\gamma n \rightarrow n\pi^0) = A^{(+)} - A^{(0)}. \tag{10}$$

If the resonances of the πN system are analysed in terms of isospin I, the three amplitudes of equation (9) have to be combined as

$$
\begin{aligned}
A^{(3/2)} &= A^{(+)} - A^{(-)} && (I = \tfrac{3}{2}) \\
A^{(1/2)} &= A^{(+)} + 2A^{(-)} && (I = \tfrac{1}{2}). \\
A^{(0)} &&& (I = \tfrac{1}{2}).
\end{aligned}
\tag{11}
$$

Neglecting isospin symmetry breaking forces, all invariants and multipole amplitudes of the preceding sections can be decomposed into the isospin amplitudes of equations (9) or (10). As an example, the dominant multipoles, the real part of E_{0+} and the imaginary part of M_{1+}, are shown in figure 5.

2.5. Cross sections and structure functions

Following the notation of Bjorken and Drell (1964), the differential cross section for an exclusive process may be written

$$
\mathrm{d}\sigma = \frac{\varepsilon_i}{k_i} \frac{m_e}{\varepsilon_i} \frac{m_i}{E_i} \frac{m_e}{\varepsilon_f} \frac{\mathrm{d}^3 k_f}{(2\pi)^3} \frac{1}{2\omega_\pi} \frac{\mathrm{d}^3 k}{(2\pi)^3} \frac{m_f}{E_f} \frac{\mathrm{d}^3 P_f}{(2\pi)^3} (2\pi)^4 \delta^{(4)}(P_i + q - k - P_f)
$$
$$
\times |\langle P_f, k| J^\mu |P_i\rangle q^{-2} \langle k_f| j_\mu |k_i\rangle|^2
\tag{12}
$$

where the phase space is evaluated in the laboratory frame and all kinematical variables are defined as in figure 3.

We have assumed a purely electromagnetic process described by the currents of the electron (j_μ) and the hadronic system (J_μ), i.e. weak neutral currents of the structure $\gamma_\mu (1 - \gamma_5)$ due to the exchange of the Z^0 have been neglected. The current of the electron is well defined in terms of Dirac spinors with normalization $\bar{u}u = 1$ and Dirac matrices γ_μ.

The cross section has to be summed and averaged over the unobserved spin degrees of freedom in the final and initial states, respectively. For simplicity we will assume that the hadronic system is unpolarized in the initial state and that the incident electron is described by a longitudinal polarization corresponding to helicity eigenstates with $h = \boldsymbol{\sigma} \cdot \hat{k}_i = \pm 1$. In both cases we will sum over all spin observables in the final state, i.e. neglect the possibility of observing recoil
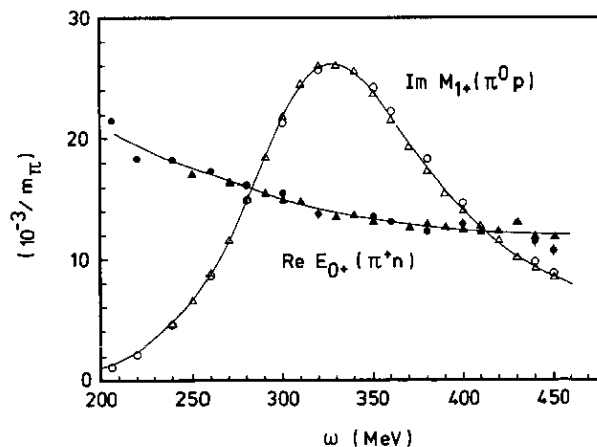

Figure 5. The dominant multipoles of pion photoproduction. The data are from Pfeil and Schwela (1972) (circles), and Berends and Donnachie (1975) (triangles).

polarization. More general polarization degrees of freedom will be discussed in section 2.6.

The square of the transition matrix elements of the currents in equation (12) may be cast into the product of two rank-2 Lorentz tensors, $\eta_{\mu\nu}$ and $W_{\mu\nu}$. The lepton tensor is easily evaluated,

$$\eta_{\mu\nu} = \sum_{s_f} (\bar{u}(k_f, s_f)e\gamma_\mu u(k_i, s_i))(\bar{u}(k_f, s_f)e\gamma_\nu u(k_i, s_i))^*$$

$$= \frac{e^2}{2m_e^2}(2K_\mu K_\nu + \tfrac{1}{2}q^2 g_{\mu\nu} - \tfrac{1}{2}q_\mu q_\nu + ih\varepsilon_{\mu\nu\alpha\beta}q^\alpha K^\beta) \tag{13}$$

with m_e the mass of the electron, $K = \tfrac{1}{2}(k_i + k_f)$, h the helicity of the incoming electron, $g_{\mu\nu}$ the (symmetrical) metric tensor and $\varepsilon_{\mu\nu\alpha\beta}$ a completely antisymmetrical tensor ($\varepsilon_{0123} = 1$). Gauge invariance is fulfilled since

$$q^\mu\eta_{\mu\nu} = \eta_{\mu\nu}q^\nu = 0.$$

The hadron tensor is defined as

$$W_{\mu\nu} = (m/4\pi W)^2 \langle\chi_f| J_\mu |\chi_i\rangle \langle\chi_f| J_\nu |\chi_i\rangle^* \tag{14}$$

where $J^\mu = (\rho, \boldsymbol{J})$ is the current operator of equations (4) and (5), and $|\chi_{i,f}\rangle$ are the Pauli spinors of the nucleon in the initial and final state, respectively. For unpolarized nucleons this expression has to be averaged and summed over the initial and final spin projection of the nucleon. The current has been normalized such that the invariant matrix element for pion photoproduction (figure 1),

$$\mathfrak{M} = -i\varepsilon^\mu J_\mu \tag{15}$$

may be evaluated acording to the conventional Feynman rules in the notation of Bjorken and Drell (1964).

It is obvious that the electromagnetic current of the hadronic system should be gauge invariant. As a consequence of approximations in treating the hadronic system on the basis of a microscopical model, gauge invariance may be lost. It is strongly recommended, therefore, to check the validity of current conservation by an explicit comparison of charges and longitudinal currents.

Figure 6 shows the kinematics for a typical coincidence experiment. We have defined our coordinate system as follows:

$$\{\hat{\boldsymbol{e}}_x = \hat{\boldsymbol{e}}_y \times \hat{\boldsymbol{e}}_z, \hat{\boldsymbol{e}}_y = (\hat{\boldsymbol{k}}_i \times \hat{\boldsymbol{k}}_f)/\sin\Theta_e, \hat{\boldsymbol{e}}_z = \hat{\boldsymbol{q}}\} \tag{16}$$

where $\Theta_e = \cos^{-1}(\hat{\boldsymbol{k}}_i \cdot \hat{\boldsymbol{k}}_f)$ is the scattering angle. Using current conservation, all timelike components of $W_{\mu\nu}$ can be replaced by spacelike ones (direction $\hat{\boldsymbol{e}}_z = \hat{\boldsymbol{q}}$).
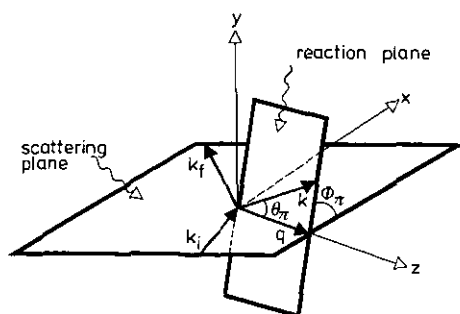

Figure 6. The kinematics for a typical coincidence experiment, leading to out-of-plane production of a pion.

The appearance of the various space directions in the tensor corresponds to the absorption of partially polarized virtual photons. This fact can be described by a degree of transverse polarization

$$\varepsilon = (1 + 2q^2/Q^2 \tan^2 \tfrac{1}{2}\Theta_e)^{-1} \tag{17}$$

where q and Θ_e are to be evaluated in the laboratory frame, and a degree of longitudinal polarization

$$\varepsilon_L = (Q^2/\omega^2)\varepsilon. \tag{18}$$

Using equations (12)–(18), we can cast the differential cross section into the following form (Amaldi *et al* 1979, Donnachie and Shaw 1978)

$$\frac{d\sigma}{d\Omega_f \, d\varepsilon_f \, d\Omega_\pi} = \Gamma \frac{d\sigma_v}{d\Omega_\pi} \tag{19}$$

$$\frac{d\sigma_v}{d\Omega_\pi} = \frac{d\sigma_T}{d\Omega_\pi} + \varepsilon_L \frac{d\sigma_L}{d\Omega_\pi} + [2\varepsilon_L(1+\varepsilon)]^{1/2} \frac{d\sigma_{TL}}{d\Omega_\pi} \cos \Phi_\pi + \varepsilon \frac{d\sigma_{TT}}{d\Omega_\pi} \cos 2\Phi_\pi$$

$$+ h[2\varepsilon_L(1-\varepsilon)]^{1/2} \frac{d\sigma_{TL'}}{d\Omega_\pi} \sin \Phi_\pi + h(1-\varepsilon^2)^{1/2} \frac{d\sigma_{TT'}}{d\Omega_\pi} \tag{20}$$

where

$$\Gamma = \frac{\alpha}{2\pi^2} \frac{\varepsilon_f}{\varepsilon_i} \frac{k_\gamma}{Q^2} \frac{1}{1-\varepsilon} \tag{21}$$

is the flux of the virtual photon field. In this expression we have introduced the 'photon equivalent energy', $k_\gamma = (W^2 - m_i^2)/2m_i$, the laboratory energy necessary for a real photon to excite a hadronic system with CM energy W. The first two terms within parentheses on the RHS of equation (20) are referred to as the transverse (T) and longitudinal (L) structure functions. They do not depend on the azimuthal angle and may be decomposed into a multipole series in $\cos \Theta_\pi$. The third term and the fifth term describe transverse–longitudinal interferences (TL and TL'), due to their dependence on $\cos \Phi_\pi$ and $\sin \Phi_\pi$ they have to contain an explicit factor $\sin \Theta_\pi$, i.e. they vanish along the axis of momentum transfer. The same is true for the fourth term, a transverse–transverse interference (TT) proportional to $\sin^2 \Theta_\pi$. The last term (TT') can only be observed by target or recoil polarization (see section 2.6).

Particularly in the case of multipole decompositions it is useful to express the angular distribution of the emitted particle in the hadronic CM frame of the final state. Therefore, equation (19) should be interpreted with the flux factor in laboratory coordinates, while the virtual photon cross sections have to be evaluated in the CM frame. For the rest of this section we will only use CM variables. The transformation of the differential cross section to the laboratory frame is given in appendix A.

The virtual photon cross sections may be expressed in terms of the hadronic tensors W_{ik} by

$$\frac{d\sigma_v}{d\Omega_\pi} = \frac{|k|}{k_\gamma^{CM}} \left(\frac{W_{xx} + W_{yy}}{2} + \varepsilon_L W_{zz} - [2\varepsilon_L(1+\varepsilon)]^{1/2} \text{Re } W_{xz} \right.$$

$$\left. + \varepsilon \frac{W_{xx} - W_{yy}}{2} + h[(2\varepsilon_L(1-\varepsilon)]^{1/2} \text{Im } W_{yz} + h(1-\varepsilon^2)^{1/2} \text{Im } W_{xy} \right) \tag{22}$$

where $k_\gamma^{CM} = (m_i/W)k_\gamma$ is the 'photon equivalent energy' in the CM frame.

A comparison of equations (20) and (22) suggests to introduce the response functions

$$R_T = \tfrac{1}{2}(W_{xx} + W_{yy}) \qquad R_L = W_{zz}$$

$$\cos \Phi_\pi R_{TL} = -\text{Re } W_{xz} \qquad \sin \Phi_\pi R_{TL'} = \text{Im } W_{yz} \qquad (23)$$

$$\cos 2\Phi_\pi R_{TT} = \tfrac{1}{2}(W_{xx} - W_{yy}) \qquad R_{TT'} = \text{Im } W_{xy}.$$

The six response functions depend on three independent variables, e.g. $R = R(Q^2, \omega_\pi, \Theta_\pi)$. An experimental separation requires a variation of the polarization of both virtual photon, ε, and electron, h, as well as a measurement for at least one non-coplanar angle $\Phi = \Phi_\pi$. The appearance of this angle in the combinations $\cos \Phi$, $\sin \Phi$ and $\cos 2\Phi$ is related to the fact that the virtual photon carries a spin of one unit of angular momentum.

The current may be decomposed into the CGLN amplitudes and further expanded into partial waves. The resulting expressions for the response functions are given in the appendices B, C and D.

While the coincidence cross section contains information on the relative phases of the multipoles, the inclusive cross section is an incoherent sum of the multipoles,

$$\sigma_v = \sigma_T + \varepsilon_L \sigma_L \qquad (24)$$

with

$$\sigma_T = \int \frac{d\sigma_T}{d\Omega_\pi} d\Omega_\pi$$

$$= 2\pi \frac{|\boldsymbol{k}|}{k_\gamma^{CM}} \sum_{l=0}^\infty (l+1)^2 [(l+2)(|E_{l+}|^2 + |M_{l+1,-}|^2) + l(|M_{l+}|^2 + |E_{l+1,-}|^2)] \qquad (25)$$

$$\sigma_L = \int \frac{d\sigma_L}{d\Omega} d\Omega_\pi = 2\pi \frac{|\boldsymbol{k}|}{k_\gamma^{CM}} \sum_{l=0}^\infty (l+1)^3 (|L_{l+}|^2 + |L_{l-}|^2). \qquad (26)$$

2.6. Polarization degrees of freedom

Polarization observables promise to become an interesting new field in pion electroproduction. The obvious advantage of such studies is the fact that many of these observables contain interference terms, making it possible to determine small, but important amplitudes in a unique way. The new generation of high duty factor, high intensity electron accelerators will provide the experimental capabilities for such investigations. Such measurements will be forthcoming in the 1 GeV range at the accelerators at Mainz (MAMI), NIKHEF-K (AmPS) and MIT/Bates and, within a few years, also at the 4–6 GeV CEBAF project.

The general formalism for coincidence and polarization experiments has been developed by Donnelly and Raskin (1986) and Raskin and Donnelly (1989). Recently, this formalism has been applied to the reaction $p(\vec{e}, e'\vec{p})\pi^0$, in order to study the structure of nucleon resonances (Lourie 1990a,b). Due to the polarization of the recoiling proton, the differential cross section contains a total of 18 structure

functions,

$$\frac{d\sigma_v}{d\Omega} = \frac{|k|}{k_\gamma^{CM}} \{ (R_T + P_n R_T^n) + \varepsilon_L (R_L + P_n R_L^n)$$

$$+ [2\varepsilon_L(1 + \varepsilon)]^{1/2}[(R_{TL} + P_n R_{TL}^n) \cos \Phi + (P_l R_{TL}^l + P_t R_{TL}^t) \sin \Phi]$$

$$+ \varepsilon[(R_{TT} + P_n R_{TT}^n) \cos 2\Phi + (P_l R_{TT}^l + P_t R_{TT}^t) \sin 2\Phi]$$

$$+ h[2\varepsilon_L(1 - \varepsilon)]^{1/2}[(R_{TL'} + P_n R_{TL'}^n) \sin \Phi + (P_l R_{TL'}^l + P_t R_{TL'}^t) \cos \Phi]$$

$$+ h(1 - \varepsilon^2)^{1/2}(P_l R_{TT'}^l + P_t R_{TT'}^t) \}. \tag{27}$$

In addition to h, the helicity of the electron, there appear the projections of the proton spin unto the three axes $\hat{n} = \hat{q} \times \hat{k} / \sin \Theta_\pi$ (normal to the reaction plane), $\hat{l}$ (along the proton momentum) and $\hat{t} = \hat{n} \times \hat{l}$. For example, $P_n = \hat{n} \cdot \hat{S}_R$ is the projection of the spin vector (in the proton rest frame!) unto the axis normal to the reaction plane.

The cross section for reactions induced by real photons follows if we (i) replace Γ by the flux factor for real photons, (ii) drop all longitudinal currents, and (iii) replace k_γ^{CM} by the energy of the real photon in the CM frame. We find

$$\frac{d\sigma}{d\Omega} = \frac{|k|}{|q|} \{ (R_T + P_n R_T^n) + \Pi_T[(R_{TT} + P_n R_{TT}^n) \cos 2\varphi - (P_l R_{TT}^l + P_t R_{TT}^t) \sin 2\varphi]$$

$$+ \Pi_C(P_l R_{TT'}^l + P_t R_{TT'}^t) \} \tag{28}$$

where Π_T is the degree of linear polarization of the real photon and φ the angle of the polarization vector relative to the reaction plane, and Π_C is the degree of circular polarization. For example, for completely linearly polarized photons with polarization vector normal to the production plane, $\Pi_T = 1$, $\varphi = \frac{1}{2}\pi$ and $\Pi_C = 0$, while right (left)-circularly polarized photons have $\Pi_T = 0$ and $\Pi_C = +1(-1)$.

In experiments with polarization degree of freedom it is common to define the following observables (Moorhouse 1978, Walker 1969):
(i) the polarized photon asymmetry

$$\Sigma(\Theta) = -R_{TT}/R_T \tag{29a}$$

(ii) the polarized target asymmetry

$$T(\Theta) = R_T(n_i)/R_T = -R_{TT}(n_f)/R_T \tag{29b}$$

(iii) the recoil nucleon polarization

$$P(\Theta) = R_T(n_f)/R_T = -R_{TT}(n_i)/R_T \tag{29c}$$

where n_i and n_f refers to the polarization of the nucleon in the initial and final state, see appendix B.

In addition there are four observables for polarization of both beam and target,

$$E(\Theta) = -R_{TT'}(l_i)/R_T \qquad F(\Theta) = R_{TT'}(t_i)/R_T$$
$$G(\Theta) = -R_{TT}(l_i)/R_T \qquad H(\Theta) = R_{TT}(t_i)/R_T. \tag{29d}$$

The corresponding four observables for polarization of beam and recoil nucleon are obtained by replacing $l_i, t_i \rightarrow l_f, t_f$ in equation (29d).

Finally one can measure four observables for polarization of target and recoil nucleon. As shown by Borke *et al* (1975) a complete experiment requires, besides
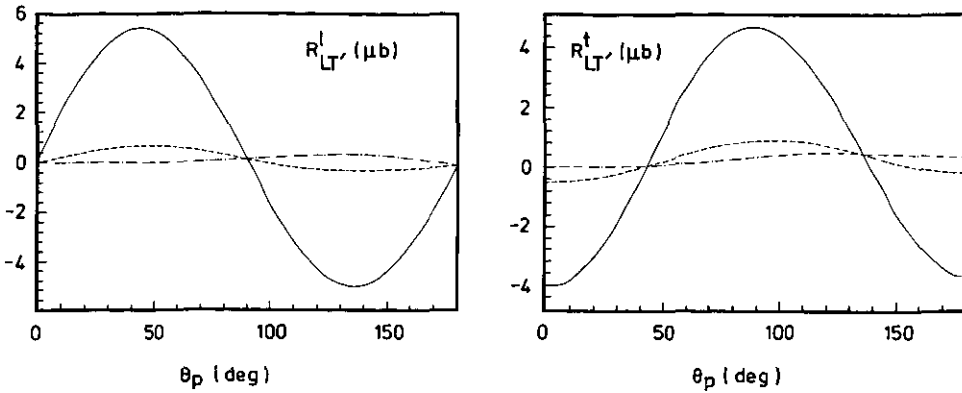
Figure 7. The dependence of the response functions $R^l_{TL'}$ and $R^t_{TL'}$ on the quadrupole amplitude L_{1+}/E_{1+} in the region of the $\Delta(1232)$. The full and chain curves show the results with and without the L_{1+}/E_{1+} multipole (for details see Lourie 1990).

the differential cross section and the three single polarization observables Σ, T and P, only five out of 12 double polarization observables.

Even an in-plane experiment allows to separate the six response functions $R_{TT'}$, $R^t_{TT'}$, $R^l_{TL'}$, $R^t_{TL'}$, R_{TL} and R^n_{TL}. In the Δ resonance region, the functions $R^t_{TL'}$, $R^t_{TT'}$ and R_{TL} are of particular importance, because they contain the interference term $L^*_{1+}M_{1+}$ and, to some degree, contributions of the non-resonant longitudinal amplitudes L_{i-} and L_{0+}. Therefore, the experiment allows to separate the resonance contribution L_{1+} ('Δ deformation') from the non-resonant background. The strength of such background contributions can also be determined from R^n_{TL}. Being the imaginary part of an interference it vanishes for an isolated resonance, i.e. it contributes only in situations of overlapping resonances or interference terms between a resonance with a background amplitude.

Figure 7 shows the dependence of the response functions $R^l_{TL'}$ and $R^t_{TL'}$ on the L_{1+}/E_{1+} amplitudes. It is clearly seen that the two latter ones are extremely sensitive to the electric quadrupole amplitude ('Δ deformation').

3. Experimental data

As will be shown in section 4, the low energy theorem (LET) predicts that the E_{0+} amplitude is strongly suppressed for neutral pions. This can also be seen in figure 8 by comparing the total cross sections for charged and neutral pion production. While the M_{1+} resonance at 300 MeV is clearly pronounced in all three channels, a strong background of E_{0+} is visible in the case of charged pions.

The theoretical predictions of LET for the E_{0+} amplitude are shown in table 4 together with some model calculations and the experimental data. While the experimental numbers for $\pi^\pm$ production have been smoothly extrapolated to threshold, the analysis of two recent experiments (Mazzucato *et al* 1986, Beck *et al* 1990) has shown that this is not possible in the case of (γ, π^0) off the proton. In the energy range of about 10 MeV above threshold the E_{0+} amplitude varies between $-1.4 \times 10^{-3}/m_\pi$ and 0. This is the reason why there is no entry in table 4. In previous publications on this subject numbers of -0.5 ± 0.3 (Mazzucato *et al* 1986) and
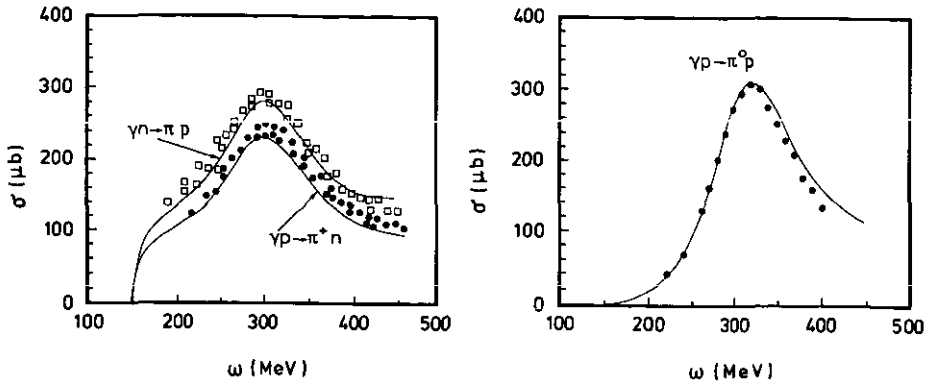
Figure 8. The total cross section for pion photoproduction as function of photon energy ω. (Data from Menze *et al* (1977) and Bagheri *et al* (1988), compared to calculations of Nozawa *et al* (1990).)

-0.35 ± 0.1 (Beck 1989) have been quoted. However, these numbers have been obtained in a highly debated model-dependent work. Therefore, they cannot be compared with the theoretical predictions of table 4. Further details on the model dependent analysis are discussed together with final state interactions in section 6.3.

As may be seen in figure 9, the threshold cross section does not show the strong S-wave contributions predicted by the theory. Instead the data essentially follow the energy dependence given by the P_{33} resonance. Similarly there is little indication of the expected 'cusp effect' in the cross section at $\omega = 151.4$ Mev, where the threshold for the competing $n\pi^+$ channel opens.

The suppression of the E_{0+} amplitude can also be seen by inspecting the angular distribution shown in figure 10 for a photon energy $\omega = 149.1$ MeV. While LET predicts a cross section peaked in the backward region due to E_{0+}/M_{1+} interference, the experimental data are much lower and nearly symmetrical about 90° due to the lack of E_{0+} strength.

In the Mainz experiment total cross sections have been measured from threshold up to 156 MeV, and five angular distributions have been taken at 146.8, 149.1, 151.4, 153.7 and 156.1 MeV, one of them is shown in figure 10. However, it is not possible to extract the multipole amplitudes out of these data without further assumptions. In a fit of only the differential cross sections Beck *et al* (1990) have obtained two solutions for the E_{0+} amplitude, giving an ambiguity at the lowest two energies. We have analysed the differential and total cross sections in a combined way under the following assumptions:

(i) only multipoles up to $l = 1$ contribute (i.e. $E_{0+}, E_{1+}, M_{1+}, M_{1-}$),

Table 4. Pion photoproduction amplitude E_{0+} in units of $10^{-3}/m_\pi$. LET, low energy theorem; PV, Born terms in pseudovector coupling; PV+, PV plus vector meson exchange ω, ρ and u-channel Δ resonance; CQM, constituent quark model (Drechsel and Tiator 1984). Experimental data from Adamovitch (1976).

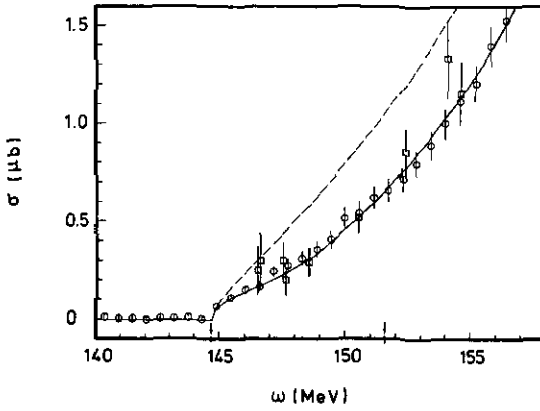| Channel	LET	PV	PV+	CQM	Experiment
$\gamma p \rightarrow n\pi^+$	27.5	27.7	27.7	29.0	28.6 ± 0.2
$\gamma n \rightarrow p\pi^-$	-32.0	-31.9	-31.6	-33.3	-31.5 ± 1.0
$\gamma p \rightarrow p\pi^0$	-2.4	-2.5	-2.3	-2.7	
$\gamma n \rightarrow n\pi^0$	0.4	0.4	0.4	0.4	

Figure 9. Total cross section for the reaction $\gamma + p \rightarrow \pi^0 + p$ as function of photon energy. Mainz data ($\square$) according to Beck *et al* (1990), Saclay data ($\bigcirc$) of Mazzucato *et al* (1986). The full curve is a fit of the experimental data while the broken curve is obtained with a constant E_{0+} of $-2.5 \times 10^{-3}/m_\pi$ and the same p-wave multipoles as for the full curve.

(ii) the energy dependence of the P-wave multipoles follows the theoretical predictions and is proportional to the product of photon and pion momenta (i.e. $E_{1+} = e_{1+}qk \times 10^{-3}/m_\pi^3$, M_{1+}, M_{1-} analogous),

(iii) the E_{0+} amplitude is fitted at each of the five differential cross sections, interpolations are performed to other energies.

In this way we have obtained a χ^2 fit of all the data with eight parameters, five values of E_{0+} and three slope parameters for P-waves. In figure 11 we show the result of our fit for E_{0+} and a combination of P-wave multipoles $M1 \equiv M_{1+} + 3E_{1+} - M_{1-}$. Our fit gives a unique solution for the multipoles and is in good agreement with solution I of Beck *et al* (1990) except for the lowest data point of E_{0+}, where our result is close to solution II.

Among the P-wave multipoles only the M_{1+} has been measured with a satisfactory precision, $M_{1+} = (8.0 \pm 0.1)qk \times 10^{-3}/m_\pi^3$. The E_{1+} and M_{1-} multipoles still have a sizeable statistical uncertainty and should be better determined in future
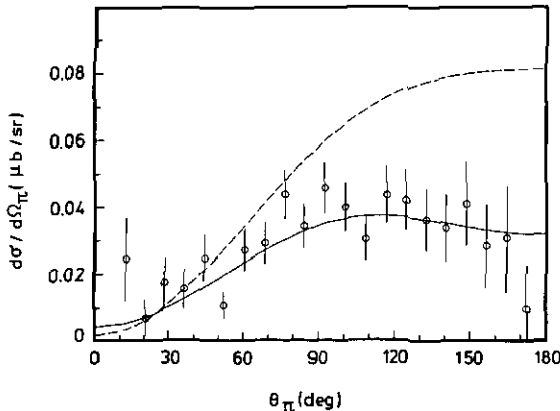

Figure 10. Angular distribution $d\sigma/d\Omega$ for $\gamma + p \rightarrow \pi + p$ at fixed photon energy $\omega = 149.1$ MeV. The broken and full curves are obtained with multipoles as in figure 9. The data are from Beck *et al* (1990).
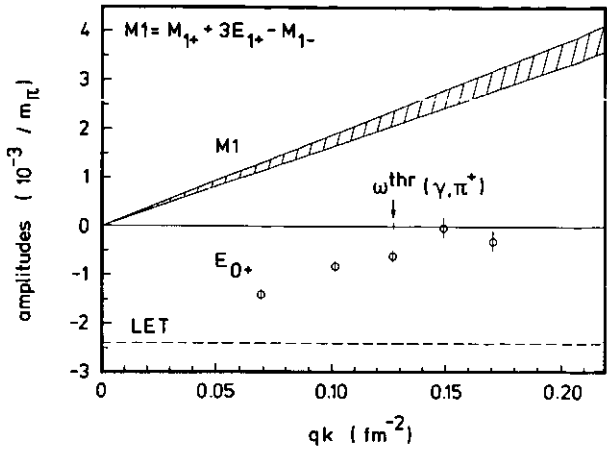
Figure 11. Result of our fit to the Mainz data. The open circles show the values of the E_{0+} amplitude and the prediction of LET is drawn as a constant over the energy range. The P-wave multipoles are given in the combination $M1 = M_{1+} + 3E_{1+} - M_{1-}$ with an error band.

Table 5. Multipole analysis of pion photoproduction at threshold. a, Adamovich (1976); b, Berends and Weaver (1971) at $\omega = 165$ MeV; c, Berends and Weaver (1971) at 180 MeV; d, Pfeil and Schwela (1972) at 180 MeV; e, Crawford and Morton (1983) at 167 MeV; f, our fit to the data of Beck *et al* (1990). Our fit of the E_{0+} amplitude as function of ω is -1.4 ± 0.1 (146.8 MeV), -0.8 ± 0.1 (149.1 MeV), -0.6 ± 0.1 (151.4 MeV), 0 ± 0.15 (153.7 MeV) and -0.3 ± 0.2 (156.1 MeV). The extrapolation to neutral pion threshold is -2.2.

	E_{0+} $(10^{-3}m_{\pi+}^{-1})$	E_{1+} $(10^{-3}qk\,m_{\pi+}^{-3})$	M_{1+} $(10^{-3}qk\,m_{\pi+}^{-3})$	M_{1-} $(10^{-3}qk\,m_{\pi+}^{-3})$	Reference
$p(\gamma, \pi^+)n$	28.6 ± 0.2				a
	26.5	4.8	-13.5	5.5	b
	24.0	4.3	-11.1	3.3	c
	25.2	3.3	-7.7	4.2	d
	24.9	4.3	-9.7	5.3	e
$n(\gamma, \pi^-)p$	-31.5 ± 1.0				a
	-29.2	-3.1	8.4	-6.0	d
	-29.1	-3.9	10.0	-6.4	e
$p(\gamma, \pi^0)p$	-2.1	-0.27	9.6	-3.9	b
	-2.2	-0.75	8.5	-3.2	c
	-1.9	$+0.12$	8.6	-0.9	d
	-1.8	-0.21	6.6	-2.5	e
		-0.50	8.0	-2.3	f
$n(\gamma, \pi^0)n$	1.0	0.13	7.8	0.5	d
	1.1	-0.21	5.9	-1.4	e

experiments with polarization degrees of freedom. A summary of the present multipole analysis is shown in table 5. Similar results for E_{0+} have been obtained by two recent analyses of the total cross section data (Bernstein and Holstein 1991, Bergstrom 1991).

Electroproduction between threshold and the first resonance region has been studied in the 70s at Frascati (Amaldi *et al* 1970), DESY (Brauel *et al* 1974), NINA (Botterill *et al* 1976), Saclay (Bardin *et al* 1977) and Bonn (Breuker *et al* 1978). In the virtual photon cross section (equation (20)) only a few structure functions have been separated, e.g. σ_{TL} and σ_{TT} by use of the azimuthal dependence on Φ_π (Breuker *et al* 1978) or σ_L and σ_T at $\Theta_\pi = 0°$ by a Rosenbluth plot. A direct determination of individual multipoles, however, has not yet been achieved in the near threshold region. The main interest in the experiments with charged pions has been to determine the nucleon axial form factor G_A from the transverse and the induced pseudoscalar G_P from the longitudinal response, the latter being related to the pion form factor F_π by pole dominance. As will be discussed at the end of section 4.2, these form factors are not fully independent but related by the requirement of gauge invariance. Therefore the extraction of these form factors is model dependent. As an example, Bardin *et al* (1977) determine the pion radius to be $r_\pi = 0.74^{+0.11}_{-0.13}$ fm as compared to the direct measurement of Amendolia *et al* (1984) who obtain 0.66 ± 0.01 fm.

4. Low energy theorems

4.1. Current algebra

Low energy theorems (LET) have been a very powerful tool to determine the threshold amplitudes for reactions involving photons and pions. Covariance, gauge invariance and the (partial) conservation of the axial current (PCAC) allow these amplitudes to be expressed in the low energy limit in terms of the global properties of the hadrons, such as their masses, magnetic moments and coupling constants. As an example the Thomson limit for the scattering of photons at threshold (energy $\omega \to 0$) is

$$\mathrm{d}\sigma/\mathrm{d}\Omega \to \tfrac{2}{3}(\alpha/m)^2$$

where $e = \sqrt{4\pi\alpha}$ and m are the total charge and mass of the struck object. The first contributions depending on the internal structure are $O(\omega^2)$ and proportional to the electric polarizability and magnetic susceptibility of the target (Low 1954, Gell-Mann and Goldberger 1954).

While these theorems are exact in the case of photons, their application to pions involves an expansion about the unphysical 'soft-pion limit' of massless pions, as a power series in $\mu = m_\pi/m_N$. Weinberg (1966) and Tomozawa (1966) were able to explain the surprisingly small S-wave phase shifts for the scattering of low energy pions within the framework of LET.

Figure 12 shows some diagrams contributing to pion photoproduction. As for any radiative process, LET assert that the threshold behaviour is determined by the Born terms (figure 12 (a)–(d)).

The leading order term, the 'Kroll–Ruderman' amplitude (Kroll and Ruderman 1954) of figure 12(d), is fixed by the gauge invariance of the electromagnetic current. The higher order terms in the mass ratio μ are determined by chiral invariance, i.e.
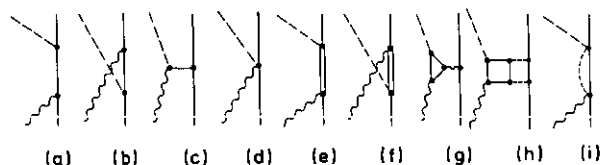
Figure 12. Diagrams contributing to pion photoproduction: (a) direct, (b) crossed nucleon pole term, (c) pion pole, (d) Kroll–Ruderman term, (e) and (f) isobar excitation, (g) triangle anomaly (photon pole, vector meson exchange), (h) square anomaly, (i) rescattering.

by the partial conservation of the axial current (PCAC). Typical model-dependent corrections are of relative order μ^2 (Fubini *et al* 1965, de Baenst 1970).

Ultimately, the vector and axial currents of the hadronic system can be expressed in terms of the quark degrees of freedom appearing in the QCD Lagrangian. On the usual energy scale of hadrons, the masses of the three lightest quarks (u, d, s) can be neglected. In this limit, we obtain eight conserved vector and axial currents,

$$J_\mu^a = \tfrac{1}{2}\bar{q}\gamma_\mu\lambda^a q \tag{30}$$

$$J_{5\mu}^a = \tfrac{1}{2}\bar{q}\gamma_\mu\gamma_5\lambda^a q. \tag{31}$$

The Gell-Mann matrices λ_a refer to the flavours of the three lightest quarks. Due to the symmetry-breaking mass matrix

$$M = \begin{pmatrix} m_u & 0 & 0 \\ 0 & m_d & 0 \\ 0 & 0 & m_s \end{pmatrix} \tag{32}$$

the currents of equations (30) and (31) have the divergence

$$\partial^\mu J_\mu^a = i\bar{q}[M, \tfrac{1}{2}\lambda^a]q \tag{33}$$

$$\partial^\mu J_{5\mu}^a = i\bar{q}\{M, \tfrac{1}{2}\lambda^a\}\gamma_5 q. \tag{34}$$

We note that the electromagnetic current,

$$J_\mu^{em} = e(J_\mu^3 + \sqrt{\tfrac{1}{3}}J_\mu^8) \tag{35}$$

is conserved, because it commutes with the diagonal mass matrix.

Neglecting the masses, we obtain 16 conserved charges,

$$Q^a = \int d^3x J_0^a(x) \tag{36}$$

$$Q_5^a = \int d^3x J_{50}^a(x). \tag{37}$$

As postulated first by Gell-Mann, the equal-time commutators (ETC) of these charges fulfil the $SU(3) \times SU(3)$ algebra (Adler and Dashen 1968)

$$[Q^a, Q^b] = if^{abc}Q^c \qquad [Q_5^a, Q_5^b] = if^{abc}Q^c \qquad [Q^a, Q_5^b] = if^{abc}Q_5^c. \tag{38}$$

Often we also assume such relations for commutators of charges and currents, i.e.

$$[Q^a, J_\mu^b(x)] = if^{abc}J_\mu^c(x) \qquad \text{etc.} \tag{39}$$

For completeness we note that there is an additional conserved vector current related to the unitary transformation $q \to \exp(i\alpha)q$. The corresponding axial current is not conserved, its divergence is proportional to a product of gluon field tensors ('$U(1)$ problem'). These two singlet currents are usually obtained from the octet currents, equations (30) and (31), by introducing a diagonal matrix $\lambda^0 = \sqrt{\tfrac{2}{3}}$.

Due to the non-linearity of QCD perturbative solutions are only justified in a high energy phase of quarks and gluons (perturbative QCD, asymptotic freedom). In this regime quarks and gluons propagate freely over (relatively!) large distances. In the realm of low-energy physics, however, the coupling is strong. The physical ground state has a complex structure and the effective degrees of freedom are carried by hadrons as realizations of quarks and gluons in this phase.

At the same time when quark pairs appear in the vacuum (quantum numbers: scalar–isoscalar), the non-linearities also lead to a strong attraction for quark pairs with the quantum numbers of the pion (pseudoscalar–isovector). This leads to the existence of massless pions ('Goldstone bosons'). The appearance of these *Goldstone pions* compensates the effects of the massive quarks and guarantees the conservation of the axial current even in the case of finite effective quark (and/or nucleon) masses.

Physical pions decay by weak interactions. Denoting the pion wavefunction with Φ^a, where a is an isospin index, the axial current of the pion coupling to the weak interactions is

$$J_{5\mu}^a(x) = f_\pi \, \partial_\mu \Phi^a \tag{40}$$

with $f_\pi = 92.6 \pm 0.2\,\text{MeV}$ (Coon and Scadron 1990) describing the experimentally observed lifetime of charged pions.

If we allow for finite 'current' quark masses m_u and m_d, also the Goldstone bosons obtain a finite mass m_π according to the relation (Gell-Mann *et al* 1968).

$$m_\pi^2 f_\pi^2 = -(m_u + m_d)\langle \bar{q}q \rangle. \tag{41}$$

The experimental numbers on the LHS of this equation are described quite nicely by the commonly accepted values $m_u \simeq 5\,\text{MeV}$, $m_d \simeq 9\,\text{MeV}$ and $\langle \bar{q}q \rangle = -(225\,\text{MeV})^3$ for the quark condensate (Gasser and Leutwyler 1982).

Since we have now introduced finite quark masses, chiral symmetry is broken. However, it is broken at the scale of the small current quark masses of a few MeV, not at the scale of the much larger effective masses.

4.2. AGW derivation of LET

While the applications of LET to pion photoproduction have followed a somewhat different path (Fubini *et al* 1965), we will now derive these theorems by a field-theoretical approach (Adler and Gilman 1966, Weisberger 1967).

To lowest order in the electromagnetic current, the S-matrix element for the reaction $\gamma(q) + N(p) \to \pi^\alpha(k) + N(p')$ is

$$S = -i \int d^4x \, e^{-iqx} \varepsilon^\mu(q\lambda) N_\gamma^{1/2} \langle N'\pi^\alpha | J_\mu^{\text{em}}(x) | N \rangle \tag{42}$$

where ε^μ is the polarization vector of the electromagnetic field, $N_\gamma = (2\pi)^{-3}(2q_0)^{-1}$ its normalization, and the hadronic systems are described by exact solutions of the Lagrangian with appropriate 'in' and 'out' boundary conditions.

On a phenomenological level, in a model with nucleons and pions, we have

$$J_\mu = J_\mu^N + J_\mu^\pi + J_\mu^{int}. \tag{43}$$

The current operators of free nucleons and pions are

$$J_\mu^N = \bar{\psi}\frac{1+\tau_0}{2}\gamma_\mu\psi + \frac{\partial^\nu}{2m}(\bar{\psi}(\kappa_s + \kappa_v\tau_0)\sigma_{\mu\nu}\psi) \tag{44}$$

$$J_\mu^\pi = (\mathbf{\Phi} \times \partial_\mu\mathbf{\Phi})_3 = \varepsilon_{\beta\gamma3}\Phi^\beta\partial_\mu\Phi^\gamma. \tag{45}$$

In particular we note that the nucleon current includes the familiar Pauli term. The derivative in this term can be removed, $\partial^\nu \to iq^\nu$, by a partial differentiation in equation (42). While the first two currents on the RHS of equation (43) are completely determined by the well known properties (Lagrangian) of free nucleons and pions, the interaction current is strongly model dependent. In the Weinberg model, e.g. there appear many additional terms containing both nucleon and pion field operators.

Equation (42) can be simplified using translation invariance

$$\langle N'\pi | J_\mu(x) | N \rangle = \exp[-i(p - p' - k)x]\langle N'\pi | J_\mu(0) | N \rangle$$

and integrating over the space variable

$$S = -i(2\pi)^4\,\delta^4(q + p - p' - k)N_\gamma^{1/2}\varepsilon^\mu\langle N'\pi^\alpha | J_\mu^{em}(0) | N \rangle. \tag{46}$$

Next we apply the reduction technique of Lehmann *et al* (1955). Assuming a local field theory and microcausality, the S matrix can be cast into the form

$$S = (2\pi)^4\,\delta^4(q + p - p' - k)N_\gamma^{1/2}N_\pi^{1/2}\int d^4x(-k^2 + m_\pi^2)$$
$$\times e^{ikx}\langle N'| T(\Phi^\alpha(x)\varepsilon \cdot J^{em}(0)) | N \rangle \tag{47}$$

where $\Phi^\alpha(x)$ is the local pion field, an exact solution of the hadronic Lagrangian, and T the time-ordering operator.

Redefining the nucleon states such that the normalization factors $N_N = (2\pi)^{-3}(E + m)/2m$ appear explicitly, the integral in equation (47) is exactly the invariant amplitude $\mathfrak{M}$ in the notation of Bjorken and Drell (1964). It would be straightforward to calculate this amplitude within the framework of a specific Lagrangian, e.g. pseudoscalar πN coupling, by evaluating 'all Feynman graphs' with the familiar rules for vertices and propagators. However, we cannot be assured that this result makes any sense because of the large value of the coupling constant.

The physical assumption to bring us closer to a reliable numerical prediction is the PCAC hypothesis,

$$\partial^\mu J_{5\mu}^a = -f_\pi m_\pi^2\Phi^a \tag{48}$$

relating the divergence of the axial current to the local pion field. The hypothesis is, more precisely, that all higer order terms (heavier mesons, $\mathbf{\Phi}^3$ terms in the Weinberg model etc) in this equation may be neglected at low energies. This enables us to rewrite the invariant amplitude as

$$\mathfrak{M} = \frac{k^2 - m_\pi^2}{f_\pi m_\pi^2}\int d^4x\,e^{ikx}\langle N'| T(\partial^\nu J_{5\nu}^\alpha(x)\varepsilon \cdot J^{em}(0)) | N \rangle. \tag{49}$$

Eliminating the differential operator by a partial integration we obtain two contributions, the first by differentiation on the plane wave, the second by differentiation on the step functions $\Theta(x_0)$ and $\Theta(-x_0)$ implicitly contained in the time ordering operator,

$$\mathfrak{M} = \frac{-k^2 + m_\pi^2}{f_\pi m_\pi^2} \int d^4x \, e^{ikx} \{ \delta(x_0) \langle N'| \, [J_{50}^\alpha(x), \, \varepsilon \cdot J^{em}(0)] \, |N\rangle$$
$$+ ik^\nu \langle N'| \, T(J_{5\nu}^\alpha(x), \, \varepsilon \cdot J^{em}(0)) \, |N\rangle \}. \tag{50}$$

The first term in this equation contains the equal-time commutator (ETC) of the axial charge and the electromagnetic current. Due to Gell-Mann's hypothesis on ETCs (see equations (38) and (39))

$$\int d^3x [J_{50}^\alpha(x), J_\mu^{em}(0)]_{x_0=0} = ie\varepsilon_{\alpha3\beta}J_{5\mu}^\beta \tag{51}$$

and this term will yield the familiar Kroll–Ruderman term, dominating the threshold production of charged pions but vanishing for neutral pions.

Unfortunately, there is still a flaw in equation (50). For physical pions $k^2 \to m_\pi^2$, and the matrix element would vanish if it were not about the pion pole term hidden in the time-ordered product. This problem is usually circumvented, more or less carefully, by evaluating the RHS of the equation in the 'soft-pion limit', $k^2 \to 0$, as a power series in m_π^2. Instead, we follow a procedure suggested by Weisberger (1967) to first evaluate the contribution of the axial current of the pion. Similar to the case of the electromagnetic current, the axial current of the hadronic system should have the (phenomenological) form

$$J_{5\nu}^\alpha = J_{5\nu}^{N,\alpha} + f_\pi \, \partial_\nu \Phi^\alpha + J_{5\nu}^{int,\alpha} \equiv f_\pi \, \partial_\nu \Phi^\alpha + \bar{J}_{5\nu}^\alpha. \tag{52}$$

Inserting this expression into equation (50) and integrating by parts once more, we find

$$\frac{f_\pi m_\pi^2}{-k^2 + m_\pi^2} \mathfrak{M} = \int d^4x \, e^{ikx} \{ \delta(x_0) \langle N'| \, [J_{50}^\alpha, \, \varepsilon \cdot J^{em}] \, |N\rangle$$
$$- i\omega_\pi f_\pi \, \delta(x_0) \langle N'| \, [\Phi^\alpha, \, \varepsilon \cdot J^{em}] \, |N\rangle + ik^\nu \langle N'| \, T(\bar{J}_{5\nu}^\alpha \varepsilon \cdot J^{em}) \, |N\rangle$$
$$+ f_\pi k^2 \langle N'| \, T(\Phi^\alpha \varepsilon \cdot J^{em}) \, |N\rangle \}. \tag{53}$$

According to equation (49) we can identify the last term on the RHS with the invariant amplitude $\mathfrak{M}$ multiplied by $f_\pi k^2/(-k^2 + m_\pi^2)$. If we combine this term with the LHS of the equation, the pole structure vanishes. The threshold amplitude in the CM frame is simply obtained by $k \to (m_\pi, 0)$, and our final result is

$$\mathfrak{M} = \frac{1}{f_\pi} \int d^4x \, e^{ikx} \{ \delta(x_0) \langle N'| \, [J_{50}^\alpha, \, \varepsilon \cdot J^{em}] \, |N\rangle$$
$$- i\omega_\pi f_\pi \delta(x_0) \langle N'| \, [\Phi^\alpha, \, \varepsilon \cdot J^{em}] \, |N\rangle + ik^\nu \langle N'| \, T(\bar{J}_{5\nu}^\alpha \varepsilon \cdot J^{em}) \, |N\rangle \}. \tag{54}$$

As has been stated before, the first term on the RHS is the Kroll–Ruderman term. The time-ordered product yields, to lowest order, the s- and u-channel Born terms in pseudovector (PV) πN coupling. According to Adler and Dothan (1966) the higher order terms of the perturbation series contribute only to higher order in m_π since the Born terms already fulfil the assumptions of LET. The second term gives rise to the *t*-channel (pion) pole term. At threshold it only contributes to pion electroproduction.

In stating that equation (54) is equivalent to PV coupling, we have tacitly assumed that

$$\tilde{J}^{\alpha}_{5\mu} = \tfrac{1}{2}\bar{\psi}\gamma_{\mu}\gamma_5\tau^{\alpha}\psi. \tag{55}$$

The matrix element of the full axial current, equation (52) between nucleon states has the structure

$$\langle p'|J^{\alpha}_{5\mu}|p\rangle = G_A\bar{u}_{p'}\gamma_{\mu}\gamma_5\frac{\tau^{\alpha}}{2}u_p + \frac{G_P}{2m}\bar{u}_{p'}(p'-p)_{\mu}\gamma_5\frac{\tau^{\alpha}}{2}u_p \tag{56}$$

with the renormalized axial coupling constant $g_A = G_A(0) = 1.261$ (Holstein 1990) and the induced pseudoscalar G_p. Assuming pion pole dominance the two form factors are related by

$$G_p(t) = \frac{4m^2}{m^2_{\pi}-t}G_A(t) \tag{57}$$

where $t = (q-k)^2 = (p'-p)^2$. Since the pion cloud is related to the pion source function,

$$(\Box + m^2_{\pi})\Phi^{\alpha} = -ig\bar{\psi}\gamma_5\tau^{\alpha}\psi \tag{58}$$

the axial coupling constant g_A is connected with the pion decay constant f_{π} by the Goldberger–Treiman relation (1958),

$$\frac{g_A}{f_{\pi}} = \frac{g}{m} = \frac{2f}{m_{\pi}}. \tag{59}$$

Using equation (51) the commutator in the first term can be expressed by the axial current, equation (56). Assuming that the interaction currents in equation (43) commute with the pion field and by using the PCAC hypothesis, also the second term can be related to the axial current. Both terms together lead to the amplitude

$$\mathfrak{M}^{(1)} = \frac{e}{2f_{\pi}}\frac{[\tau_{\alpha},\tau_0]}{2}\bar{u}_{p'}\left\{G_A\not\epsilon + \frac{G_P}{2m}\epsilon\cdot(q-k) - \frac{\epsilon\cdot k}{m^2_{\pi}}\left(2mG_A + \frac{t}{2m}G_P\right)\right\}\gamma_5 u_p. \tag{60}$$

With equations (57) and (59) we obtain

$$\mathfrak{M}^{(1)} = e\frac{f}{m_{\pi}}\frac{[\tau_{\alpha},\tau_0]}{2}\frac{G_A(t)}{G_A(0)}\bar{u}_{p'}\left\{\not\epsilon + \frac{2m}{t-m^2_{\pi}}[\epsilon\cdot(2k-q)]\right\}\gamma_5 u_p. \tag{61}$$

While the result is essentially model independent, the time-ordered product in equation (54) can only be expressed as a perturbation series. Evaluated to leading order it gives the nucleon pole terms,

$$\mathfrak{M}^{(2)} = \frac{ef}{m_{\pi}}\frac{[\tau_{\alpha},\tau_0]}{2}\frac{G_A(k^2)}{G_A(0)}\bar{u}_{p'}\left\{F^v_1(q^2)\left(-\not\epsilon + m\left(\frac{2\epsilon\cdot p + \not q\not\epsilon}{2q\cdot p + q^2} + \frac{2\epsilon\cdot p' - \not\epsilon\not q}{q\cdot p' - q^2}\right)\right)\right.$$

$$+ F^v_2(q^2)\left(-\not\epsilon + \frac{\not q}{2}\left(\frac{2\epsilon\cdot p + \epsilon\cdot q}{2q\cdot p + q^2} + \frac{2\epsilon\cdot p' - \epsilon\cdot q}{2q\cdot p' - q^2}\right)\right.$$

$$\left.\left. + \frac{m}{2}(\not q\not\epsilon - \not\epsilon\not q)\left(\frac{1}{2q\cdot p + q^2} + \frac{1}{2q\cdot p' - q^2}\right)\right)\right\}\gamma_5 u_p$$

$$+ \frac{ef}{m_{\pi}}(\delta_{\alpha 0}\delta_{I,v} + \tau_{\alpha}\delta_{I,s})\frac{G_A(k^2)}{G_A(0)}\bar{u}_{p'}\left\{F^1_1(q^2)m\left(\frac{2\epsilon\cdot p + \not q\not\epsilon}{2q\cdot p + q^2} - \frac{2\epsilon\cdot p' - \not\epsilon\not q}{2q\cdot p' - q^2}\right)\right.$$

$$+ F_2^I(q^2)\Bigg(\frac{\not\epsilon}{2}\left(\frac{2\varepsilon\cdot p+\varepsilon\cdot q}{2q\cdot p+q^2}-\frac{2\varepsilon\cdot p'-\varepsilon\cdot q}{2q\cdot p'-q^2}\right)$$

$$+(\not q\not\epsilon-\not\epsilon\not q)\left(\frac{1}{4m}+\frac{m}{2}\left(\frac{1}{2q\cdot p+q^2}-\frac{1}{2q\cdot p'-q^2}\right)\right)\Bigg)\Bigg\}\gamma_5 u_p. \tag{62}$$

In deriving this result we have introduced the finite structure of the nucleon by multiplying the currents of equations (44) and (55) by the appropriate form factors F_1, F_2 and G_A, respectively.

Replacing ε by q in equations (61) and (62) gives the 4-divergence of the electromagnetic current, $D = iq\cdot J^{em}$, with

$$D = -e\frac{f}{m_\pi}\frac{[\tau_\alpha,\tau_0]}{2}\bar{u}_p\not{k}\gamma_5 u_p\frac{G_A((q-k)^2)-G_A(k^2)F_1^v(q^2)}{G_A(0)}. \tag{63}$$

Obviously, gauge invariance is violated if the contact terms and the nucleon pole terms are evaluated with phenomenological form factors. The reason is that these terms are treated to different order of the perturbation theory, i.e. exactly for the contact terms and to first order in the nucleon pole terms. In the case of threshold photoproduction, the arguments of the form factors are of order m_π^2, and the most consistent approach is to neglect the form factors completely. The inconsistency is more severe for electroproduction, even in the soft-pion limit ($k^2 = 0$). According to equation (63) gauge invariance would require that the axial radius r_A is equal to the isovector Dirac radius r_1^v. The experimental numbers are $r_A = 0.65 \pm 0.07$ fm and $r_1^v = 0.78 \pm 0.01$ fm. A direct calculation of the pion pole term, on the other hand, gives a contribution proportional to $F_\pi(q^2)$ with a radius $r_\pi = 0.66 \pm 0.01$ fm, very close to the axial radius. At large momentum transfer, however, the pion is described by a monopole form while the nucleon form factors follow a dipole fit (Brodsky and Chertok 1976).

The photoproduction amplitude at threshold ($k = k^{CM} = 0$) can be evaluated from equations (61) and (62) as a power series in $\mu = m_\pi/m_N$. Both form factors and higher order terms only contribute to relative $O(\mu^2)$ and will be neglected. Only the E_{0+} multipole of equation (8) and, hence, only the amplitude F_1 of equation (4) contribute to the current. Further using equation (9), the non-vanishing isospin amplitudes at threshold are given by

$$E_{0+}^{(-,+,0)} = \frac{e}{4\pi}\frac{f}{m_\pi}\frac{1}{1+\mu}A^{(-,+,0)}$$

with

$$A^{(-)} = 1 + O(\mu^2)$$
$$A^{(+,0)} = -\tfrac{1}{2}\mu + \tfrac{1}{2}\mu^2\mu_N^{(V,S)} + O(\mu^3) \tag{64}$$

where $\mu_N^{(S,V)} = \tfrac{1}{2}(\mu_p \pm \mu_n) = (0.44, 2.35)$ are the isoscalar and isovector magnetic moments of the nucleon. The amplitude $A^{(-)}$ is given by the first commutator in equation (54). It can be obtained from the seagull term of a pseudovector Lagrangian (figure 12(d)). The term of order μ in the amplitudes $A^{(+,0)}$ originates from the Dirac current in equation (62) and corresponds to antinucleons in the intermediate state, while the term of order μ^2 is a contribution from the Pauli current with intermediate nucleon states (figure 12(a) and (b)). The pion pole term (figure 12(c)) leads to a purely longitudinal current at threshold and the residual diagrams of figure 12 are of higher order in μ.

Suppose now that there is an additional induced pseudoscalar at the level of the current operator, equation (55):

$$\bar{J}_{5\mu}^{\alpha} = \bar{\psi}\gamma_{\mu}\gamma_{5}\frac{\tau^{\alpha}}{2}\psi - \frac{g_{p}}{2m}i\,\partial_{\mu}\left(\bar{\psi}\gamma_{5}\frac{\tau^{\alpha}}{2}\psi\right). \tag{65}$$

Similar to the case of the Pauli coupling for the electromagnetic current operator in equation (44), we have assumed that there is a derivative coupling at the operator level. While parts of the magnetic moments are of pionic origin and have to be renormalized to appropriate order, it seems obvious that these moments cannot be fully explained by pionic degrees of freedom. In a similar way the additional pseudoscalar in equation (65) indicates the possibility that a (probably small) part of the total induced pseudoscalar G_{p} could be of non-pionic origin.

The immediate consequence of the induced pseudoscalar in equation (65) is the appearance of a further derivative under the time ordering operator in equation (54). Another partial integration leads to an additional commutator resembling very closely the structure of the 'sigma term' discussed in section 4.3. If we choose, e.g., $g_{p} = -1$, the Goldberger–Treiman relation is changed only at the per cent level. This small change is sufficient, however, to cancel the terms of order m_{π} and to suppress E_{0+} for π^{0} production on the proton.

The current of equation (65) could be possibly realized in an extended PV model with an interaction Lagrangian

$$L^{\text{int}} = \frac{f}{m_{\pi}}\left(\bar{\psi}\gamma_{\mu}\gamma_{5}\boldsymbol{\tau}\psi - \frac{g_{p}}{2m}i\,\partial_{\mu}(\bar{\psi}\gamma_{5}\boldsymbol{\tau}\psi)\right)\cdot\partial^{\mu}\boldsymbol{\Phi}. \tag{66}$$

It is obvious that minimal coupling of the electromagnetic current will also lead to an additional contact term, as required by the gauge invariance of the theory.

Another interesting aspect of the model is that it has no effect on the reaction $\gamma + n \to \pi^{0} + n$, quite contrary to the model of Furlan $et\ al$ (see section 4.3). Therefore, the leading contribution for the neutron will still arise from its magnetic moment, in accordance with the general spirit of LET.

4.3. FPV derivation of LET

Following the work of Furlan $et\ al$ (1972, 1974) we introduce the operator

$$Q_{5L}^{\alpha} = Q_{5}^{\alpha} + \frac{i}{m_{\pi}}\dot{Q}_{5}^{\alpha} \tag{67}$$

having the matrix elements

$$\langle \pi^{\beta}|\,Q_{5L}^{\alpha}\,|0\rangle = 0$$
$$\langle 0|\,Q_{5L}^{\alpha}\,|\pi^{\beta}\rangle = 2\langle 0|\,Q_{5}^{\alpha}\,|\pi^{\beta}\rangle = -2if_{\pi}m_{\pi}(2\pi)^{3}\delta^{3}(k)\,e^{-im_{\pi}t}\delta_{\alpha\beta}. \tag{68}$$

Using the PCAC relation (48) and Gauss's law, the time derivative of the axial charge is related to the pion wavefunction, and equation (54) may be cast into the form

$$\langle N'|\,[Q_{5L}^{\alpha}\cdot\varepsilon\cdot J^{\text{em}}]\,|N\rangle = f_{\pi}\mathfrak{M} - im_{\pi}\int dt\,e^{im_{\pi}t}\langle N'|\,T(\bar{Q}_{5}^{\alpha}\varepsilon\cdot J^{\text{em}})\,|N\rangle - \text{HOT}. \tag{69}$$

Next, Furlan *et al* evaluate the commutator of Q_{5L}^{α} and J_{μ}^{em}, first by a direct calculation and second by saturating the commutator with a complete set of intermediate states $(\pi, N, \pi N, \dots)$.

$$
\begin{aligned}
\langle b | [Q_{5L}^{\alpha}, \varepsilon \cdot J^{em}] | a \rangle =& \sum_{\pi} (\langle 0 | Q_{5L}^{\alpha} | \pi^{\alpha} \rangle \langle b\pi^{\alpha} | \varepsilon \cdot J^{em} | a \rangle \\
& - \langle b | \varepsilon \cdot J^{em} | a\pi^{\alpha} \rangle \langle \pi^{\alpha} | Q_{5L}^{\alpha} | 0 \rangle) \\
& + \sum_{N} (\langle b | Q_{5L}^{\alpha} | N \rangle \langle N | \varepsilon \cdot J^{em} | a \rangle - \text{CT}) \\
& + \sum_{n \neq N, \pi} (\langle b | Q_{5L}^{\alpha} | n \rangle \langle n | \varepsilon \cdot J^{em} | a \rangle - \text{CT}).
\end{aligned}
\tag{70}
$$

In the first sum on the RHS we find the matrix elements of the electromagnetic current for both photoproduction $(a \to b\pi^{\alpha})$ and radiative capture $(a\pi^{\alpha} \to b)$. Due to the definition of Q_{5L}^{α}, equation (68), the pionic matrix element accompanying radiative capture vanishes, and is straightforward to show that the insertion of one-pion states leads directly to the photoproduction matrix elements $f_{\pi}\mathfrak{M}$ on the RHS of equation (69). Similarly the insertion of one-nucleon states (positive *and* negative energy states!) results in the second term on the RHS of that equation.

Up to this point there is no difference between the canonical derivation of LET, section 4.2, and the work of Furlan *et al*. The discrepancies appear, however, if the symmetry breaking is expressed at the microscopical level by the quark mass matrix,

$$
\dot{Q}_5^{\alpha} = i[H, Q_5^{\alpha}] = \int d^3r \, \partial^{\mu} J_{5\mu}^{\alpha} = i \int d^3r \bar{\psi}_{P'} \gamma_5 \{M, \tfrac{1}{2}\lambda^{\alpha}\} \psi_P.
\tag{71}
$$

The commutator of this quantity with the electromagnetic current is

$$
[\dot{Q}_5^{\alpha}, \rho^{em}] = -\varepsilon_{\alpha 3\beta} \bar{\psi}_{P'} (\not{p}' - \not{p}) \gamma_5 \tfrac{1}{2} \tau^{\beta} \psi_P
\tag{72}
$$

$$
[\dot{Q}_5^{\alpha}, J_i^{em}] = i m_0 (\delta_{\alpha 3} + \tfrac{1}{3}\tau_{\alpha}) \varepsilon_{ikl} \bar{\psi}_{P'} \sigma_{kl} \psi_P
\tag{73}
$$

where $m_0 = \tfrac{1}{2}(m_u + m_d)$ is the average light quark mass and $\bar{\psi}_{P'}$, ψ_P are quark spinors. While the RHS of equation (72) may still be related to the pion source function leading to the pion pole contribution of equation (60), the tensor form factor σ_{kl} of equation (73) does not appear in the field-theoretical derivation. In chiral models of pions and nucleons as well as in the σ-model, $\dot{Q}_5$ is proportional to the pion field and therefore the commutator, equation (73), vanishes (Kamal 1991, Bernstein and Holstein 1991). In analogy to pion–nucleon scattering, the additional contribution to E_{0+} arising from equation (73) has been called the 'sigma term'. As a commutator of $\dot{Q}_5$ and a spatial component of the current, it is extremely model dependent and cannot be safely evaluated on the basis of current algebra. In fact in a complete model calculation, e.g. on the basis of the QCD Lagrangian, there could (and probably will) be so-called Schwinger terms cancelling the 'tensor form factor' in equation (73). In a quark shell model of the nucleon, with symmetrical S wavefunctions, $q = N(f, i g\sigma \cdot \hat{r})^{T}$, and using the Goldberger–Treiman relation, Nath and Singh (1989) have obtained the following contributions for the chiral symmetry breaking (CSB) terms to the isospin amplitudes

$$
A_{(CSB)}^{(-)} = 0 \qquad A_{(CSB)}^{(+)} = 2\eta m_0/m_{\pi} \qquad A_{(CSB)}^{(0)} = \tfrac{10}{9}\eta m_0/m_{\pi}
\tag{74}
$$

where

$$
\eta = \tfrac{3}{5} \int (f^2 + \tfrac{1}{3}g^2) r^2 \, dr \Big/ \int (f^2 - \tfrac{1}{3}g^2) r^2 \, dr = (1 + \tfrac{3}{5}G_A)/2G_A \sim 0.7.
\tag{75}
$$

Up to this point we have assumed that the two light quarks have the same current mass m_0. Obviously, this is not the case and the mass splitting δm is of the same order as the masses themselves. As a consequence the isospin symmetry expressed in equation (9) will be broken by the 'sigma term', and the amplitude $A^{(+)}$ in equation (72) would have to be replaced by (Tiator and Drechsel 1989)

$$A^{(+)}_{(\text{ISB})} = 2\eta \frac{m_0}{m_\pi} \left(1 + \frac{\delta_m}{2m_0} \frac{1 + 5\tau_3}{3}\right). \tag{76}$$

The resulting corrections are quite large for neutral pions. In particular they nearly cancel the leading order term for the $p\pi^0$ amplitude. It is even more surprising that the leading term for $n\pi^0$ now stems from convection currents of the quarks!

In a recent extension of this work, Schäfer and Weise (1991) have found a strong model dependence of this effect in a chiral model with a pion cloud surrounding the quark bag. In particular, the additional term decreases strongly with the radius of the quark bag. It is interesting to note that the size of the effect is related, in this model, to the strength of the singlet axial coupling constant responsible for the 'spin crisis' in deep inelastic lepton scattering.

While the idea of Furlan *et al* may explain some of the discrepancies between LET and the data, there are some serious flaws connected with it. In particular,
(i) the additional term in equation (73) is not gauge invariant,
(ii) there is no motivation for the additional term in a field-theoretical derivation of LET,
(iii) it results from a highly model-dependent commutator relation, and
(iv) the leading term for the neutral system $n\pi^0$ is no longer the magnetic moment but the convection current of the constituents.

5. Models of pions and nucleons

5.1. Phenomenological models

On the phenomenological basis, the first theory of nucleons and pions was formulated with a pseudoscalar (PS) coupling. Such a theory can be renormalized. However, we realize now that this model does not obey the PCAC relation. The Lagrangian is given by terms describing the free nucleon, the free proton and the PS interaction,

$$\mathscr{L} = \bar{\psi}(i\not{\partial} - m)\psi + \tfrac{1}{2}(\partial^\mu \boldsymbol{\Phi} \cdot \partial_\mu \boldsymbol{\Phi} - m_\pi^2 \boldsymbol{\Phi} \cdot \boldsymbol{\Phi}) + \mathscr{L}^{\text{PS}}_{\text{int}} \qquad \mathscr{L}^{\text{PS}}_{\text{int}} = -ig\bar{\psi}\gamma_5\boldsymbol{\tau}\psi \cdot \boldsymbol{\Phi}. \tag{77}$$

The equations of motion derived from this Lagrangian are

$$(i\not{\partial} - m)\psi = ig\gamma_5\boldsymbol{\tau} \cdot \boldsymbol{\Phi}\psi \qquad (\Box + m_\pi^2)\Phi^\alpha = -ig\bar{\psi}\gamma_5\tau^\alpha\psi. \tag{78}$$

It can be shown that $\mathscr{L}$ is invariant under the infinitesimal transformations

$$U(1): \quad \psi \rightarrow (1 - i\varepsilon)\psi$$
$$SU(2): \quad \psi \rightarrow (1 - \tfrac{1}{2}i\boldsymbol{\tau} \cdot \boldsymbol{\varepsilon})\psi \qquad \text{and} \qquad \boldsymbol{\Phi} \rightarrow \boldsymbol{\Phi} + \boldsymbol{\varepsilon} \times \boldsymbol{\Phi} \tag{79}$$

leading to the conserved isoscalar and isovector components of the electromagnetic current,

$$J^{\text{em}}_\mu = \tfrac{1}{2}\bar{\psi}\gamma_\mu(1 + \tau_3)\psi + (\boldsymbol{\Phi} \times \partial_\mu \boldsymbol{\Phi})_3. \tag{80}$$

However, the (isovector) axial current is not conserved. The transformation

$$SU(2): \quad \psi \to (1 - \tfrac{1}{2}\boldsymbol{\tau} \cdot \boldsymbol{\varepsilon} \gamma_5)\psi \qquad \text{and} \qquad \boldsymbol{\Phi} \to \boldsymbol{\Phi} + f_\pi \boldsymbol{\varepsilon} \tag{81}$$

leads to

$$\mathscr{L}' - \mathscr{L} = \boldsymbol{\varepsilon} \cdot (-m_\pi^2 f_\pi \boldsymbol{\Phi} + \mathrm{i}(m - f_\pi g)\bar\psi \gamma_5 \boldsymbol{\tau}\psi - g\bar\psi\psi\boldsymbol{\Phi}). \tag{82}$$

While the first term on the RHS has the right structure, the other two terms violate PCAC. The second one can be removed by an appropriate choice of the coupling constants. Except for renormalization effects of the axial coupling constant, $g_A \neq 1$, it vanishes due to the Goldberger–Treiman relation, equation (59). However, PS coupling does not fulfil PCAC due to the last term in equation (82). As a consequence a calculation of the Born terms with PS coupling gives a result differing from equation (64) in the magnetic moment terms.

A competing model contains a gradient or pseudovector (PV) coupling,

$$\mathscr{L}_{\mathrm{int}}^{\mathrm{PV}} = \frac{f}{m_\pi} \bar\psi \gamma_\mu \gamma_5 \boldsymbol{\tau}\psi \cdot \partial^\mu \boldsymbol{\Phi}. \tag{83}$$

If we require that pion production by an on-shell nucleon has the same strength in both cases,

$$\frac{f}{m_\pi} = \frac{g}{2m} \simeq \frac{1}{2f_\pi} \tag{84}$$

the somewhat unsymmetrical transformation

$$SU(2): \quad \psi \to \psi \qquad \text{and} \qquad \boldsymbol{\Phi} \to \boldsymbol{\Phi} + f_\pi \boldsymbol{\varepsilon} \tag{85}$$

leads to the appropriate axial current

$$J_{5\mu}^{\mathrm{a}} = \bar\psi \gamma_\mu \gamma_5 \tfrac{1}{2}\tau^{\mathrm{a}}\psi + f_\pi \, \partial_\mu \Phi^{\mathrm{a}} \tag{86}$$

fulfilling the PCAC relation.

A more satisfactory PS theory can be derived from equation (83) by a redefinition of the baryon field,

$$\psi = \exp\!\left(\mathrm{i}\, \frac{f}{m_\pi} \boldsymbol{\tau} \cdot \boldsymbol{\Phi}\gamma_5 \right) \bar\psi \tag{87}$$

leading back to the PS coupling of equation (77) *plus* higher order interaction terms. In particular we obtain the additional interaction (Fubini *et al* 1965)

$$L_{\pi NN\gamma} = \mathrm{i}\, \frac{f}{m_\pi} \frac{eF^{\mu\nu}}{4m} \bar\psi \sigma_{\mu\nu} \{\kappa_s + \tau_0 \kappa_v, \, \boldsymbol{\tau} \cdot \boldsymbol{\Phi}\} \gamma_5 \psi \tag{88}$$

where $F^{\mu\nu}$ is the electromagnetic field tensor and $\kappa_{s/v}$ are the isoscalar and isovector anomalous magnetic moments of the nucleon. Since the Lagrangian is now equivalent to PV coupling, such a modified PS theory fulfils LET.

Unfortunately, the PV model cannot be renormalized. Moreover, the transformation of equation (85) is against the spirit of considering both nucleons and pions under local transformation involving the isospin. A model improving the situation and, at the same time, giving a very exact description of S- and P-wave pion scattering on nucleons, is the Weinberg model (1967),

$$\mathscr{L}_{\mathrm{int}}^{\mathrm{W}} = \frac{f}{m_\pi} \bar\psi \gamma_\mu \gamma_5 \boldsymbol{\tau}\psi \cdot \partial^\mu \boldsymbol{\Phi} + \frac{f_0^2}{m_\pi^2} \bar\psi \gamma^\mu \boldsymbol{\tau}\psi \cdot (\partial_\mu \boldsymbol{\Phi} \times \boldsymbol{\Phi}) \tag{89}$$

with $f^2/4\pi = 0.08$ and $f_0 \simeq 0.84$ fixed by the experimental scattering lengths for P and S waves, respectively. Due to the non-linearity in the second term of equation (89), the (conserved) vector currents and the (partially conserved) axial currents now contain interaction terms in addition to the currents of free pions and nucleons (equations (80) and (86)). In particular, the RHS of the PCAC relation (48) now contains terms of order Φ^3.

5.2. Constituent quark model

Non-relativistic quark models have been successfully applied to the excited states of the nucleon and their coupling to photons and pions (Isgur and Karl 1978, Copley *et al* 1969, Koniuk and Isgur 1980). With a harmonic oscillator potential describing the confinement, the problem of spurious CM motion can be avoided, leading to 'the right degrees of freedom moving at the wrong speed'. An additional hyperfine force, a residual interaction of gluon exchange between the quarks, mixes the harmonic oscillator orbits and leads to a realistic splitting of the oscillator multiplets.

In order to obtain LET, the PV Lagrangian, equation (83), has to be evaluated half off-shell, leading to both intermediate quark–antiquark states ($q\bar{q}$, Z-graphs) and positive energy contributions. The Z-graphs are evaluated by using closure over the negative energy spectrum, approximating the propagator by the mass of the quark pair. The positive energy intermediate states include the dipole excitations of the nucleon, S_{11} (1535), $S'_{11}(1650)$ and S_{31} (1650). The photoproduction amplitude can be analytically evaluated and expanded as a power series in the mass ratio μ. The various contributions to the S-wave amplitude near threshold are shown in table 6 (Drechsel and Tiator 1984). Due to the PV coupling the Kroll–Ruderman term is directly obtained from the seagull graph.

Concerning the amplitude $A^{(+)}$, both backward ('Z') and forward ('dipole') propagating states contribute to leading order in μ. Only the sum of these two terms gives the result required by LET. We recall that in a model of structureless nucleons (section 4.2) the same contribution was obtained from Z-graphs only, i.e. intermediate nucleon–antinucleon states. The situation is particularly delicate for the reaction $\gamma n \rightarrow n\pi^0$, where the convection currents $O(\mu)$ cancel and only the term $O(\mu^2\mu_n)$ remains. Obviously the existence of charged constituents can manifest itself

Table 6. Predictions of the constituent quark model with pseudovector quark–pion coupling for the S-wave amplitudes defined by equation (64). The pion–nucleon mass ratio is denoted by μ, while $\mu_{s/v} = \frac{1}{2}(\mu_p \pm \mu_n)$ are the isoscalar and isovector magnetic moments of the nucleon and α_0 is the oscillator parameter.

Contribution	$A^{(-)}$	$A^{(0)}$	$A^{(+)}$
Seagull	1	0	0
Z	$\frac{9}{10}\mu^2\mu_v$	$-\frac{1}{2}\mu$	$-\frac{9}{10}\mu$
Dipole	$\frac{1}{3}\mu^2 m^2/\alpha_0^2$	$[\mu^3]$	$\frac{2}{5}\mu$
N	$-\frac{1}{2}\mu^2\mu_v$	$\frac{1}{2}\mu^2\mu_s$	$\frac{1}{2}\mu^2\mu_v$
Δ	$-\frac{4}{25}\mu^2\mu_v$	0	$-\frac{8}{25}\mu^2\mu_v$
LET	$1 + [\mu^2]$	$-\frac{1}{2}\mu + \frac{1}{2}\mu^2\mu_s + [\mu^3]$	$-\frac{1}{2}\mu + \frac{1}{2}\mu^2\mu_v + [\mu^3]$

only to $O(\mu^3)$. In order to obtain this cancellation required by LET it is prerequisite to treat all contributions on the basis of the same Lagrangian, i.e.
(i) the wavefunctions of the excited states should be compatible with the ground state wavefunction (e.g. no phenomenological form factors!),
(ii) the excited spectrum should be complete and spurious CM motions have to be removed.

We note in passing that LET also requires the existence of a non-degenerate ground state. If we introduce the usual hyperfine interaction, the degeneracy of the nucleon (N) and its first resonance (Δ) is removed and the Δ contributions in table 6 appear as higher order terms in μ.

5.3. Bag models

Following earlier ideas of Bogoliubov, the relativistic MIT bag model was formulated by Chodos *et al* (1974). Its Lagrangian

$$L^{\mathrm{MIT}} = \left(\sum \bar{q}(\mathrm{i}\not{\partial} - m_q)q - B\right)\Theta_\mathrm{v} - \tfrac{1}{2}\sum \bar{q}q\,\Delta_\mathrm{s} \qquad (90)$$

consists of Dirac particles moving inside a bag described by the step function Θ_v. In addition, there is a bag pressure leading to a volume energy $\sim B$ and a surface term described by the surface delta function Δ_s. The solutions of this Lagrangian are spherical Bessel functions with wavenumbers quantized by the boundary condition

$$n^\mu \bar{q}\gamma_\mu q\,\Delta_\mathrm{s} = 0$$

i.e. the component of the current in the direction of n_μ, perpendicular to the bag surface, vanishes.

It is straightforward to derive that the isovector and isoscalar components of the electromagnetic current are conserved. However, the axial current, equation (55), is not even conserved in the limit $m_q \to 0$, because the boundary condition corresponds to an effective mass term. At this boundary the particles are reflected and the helicity is changed, leading to a source of the 4-divergence of the axial current at the surface.

In order to allow for a conservation of helicity, isoscalar (σ) and isovector (π) mesons have to be introduced in addition to the quarks. The Lagrangian of these σ models has the typical structure (Chodos and Thorn 1975)

$$L^\sigma = \left(\mathrm{i}\sum \bar{q}\not{\partial}q - B\right)\Theta_\mathrm{v} + \tfrac{1}{2}(\partial_\mu\sigma)^2 + \tfrac{1}{2}(\partial_\mu\pi)^2 - \sum \bar{q}\frac{\sigma + \mathrm{i}\boldsymbol{\tau}\cdot\boldsymbol{\pi}\gamma_5}{2(\sigma^2 + \pi^2)^{1/2}}q\,\Delta_\mathrm{s}. \qquad (91)$$

In this way the surface term of L^{MIT} has been replaced by a surface interaction of the quarks with the σ and π fields, in a 'chiral' combination. This Lagrangian is now invariant under the combined transformation

$$q \to (1 - \tfrac{1}{2}\mathrm{i}\boldsymbol{\tau}\cdot\boldsymbol{\varepsilon}\gamma_5)q \qquad \sigma \to \sigma - \boldsymbol{\varepsilon}\cdot\boldsymbol{\pi} \qquad \boldsymbol{\pi} \to \boldsymbol{\pi} + \sigma\boldsymbol{\varepsilon}$$

leading to a conserved (isovector) axial current

$$J^\mathrm{a}_{5\mu} = \tfrac{1}{2}\bar{q}\gamma_\mu\gamma_5\tau^\mathrm{a}q\Theta_\mathrm{v} - \pi^\mathrm{a}\,\partial^\mu\sigma + \sigma\,\partial^\mu\pi^\mathrm{a}. \qquad (92)$$

Since the σ field does not appear as a physical meson, it is often eliminated by the relation $\sigma^2 + \pi^2 = f_\pi^2$ ('non-linear σ model').

In the 'cloudy bag model' the physical pion Φ is related to the original boson fields by the equations

$$\pi = f_\pi \hat{\boldsymbol{\Phi}} \sin(\Phi/f_\pi) \qquad \sigma = f_\pi \cos(\Phi/f_\pi).$$

The Lagrangian of the 'non-linear' cloudy-bag model is (Thomas 1984)

$$L^{\text{CBM}} = \left(i \sum \bar{q} \not{\partial} q - B \right) \Theta_v - \tfrac{1}{2}\bar{q} \exp(i\boldsymbol{\tau} \cdot \boldsymbol{\Phi} \gamma_5/f_\pi)q \, \Delta_s + \tfrac{1}{2}(D_\mu \boldsymbol{\Phi})^2 - \tfrac{1}{2}m_\pi^2 \boldsymbol{\Phi}^2 \tag{93}$$

where D_μ is the covariant derivative

$$D_\mu \boldsymbol{\Phi} = (\partial_\mu \Phi)\hat{\boldsymbol{\Phi}} + f_\pi \sin(\Phi/f_\pi) \, \partial_\mu \hat{\boldsymbol{\Phi}}.$$

In order to obtain the PCAC relation, a pion mass term has been added to L^{CBM}.

In the case of small fluctuations of the pion field, equation (93) may be expanded in Φ. Keeping only the lowest order terms, we obtain the Lagrangian of the linearized cloudy-bag model with PS coupling at the bag surface (Kälbermann and Eisenberg 1983)

$$\mathscr{L}^{\text{PS}} = \mathscr{L}^{\text{MIT}} + \tfrac{1}{2}(\partial_\mu \boldsymbol{\Phi})^2 - \tfrac{1}{2}m_\pi^2 \boldsymbol{\Phi}^2 - \frac{i}{2f_\pi} \bar{q}\gamma_5 \boldsymbol{\tau} \cdot \boldsymbol{\Phi} q \, \Delta_s. \tag{94}$$

While CBMS conserve the electromagnetic current and generally fulfil the PCAC relation, their solutions are based on relativistic shell model wavefunctions for the three valence quarks. Therefore, the problem of spurious CM motion arises. In particular the spectrum of intermediate states entering into a calculation of threshold pion photoproduction contains spurious dipole oscillations of the CM.

Using pseudovector coupling and relativistic bag wavefunctions for massless quarks, Scherer *et al* (1987) have calculated the S-wave amplitude E_{0+} at threshold. They have shown explicitly that the contributions stemming from intermediate valence quark excitations ($n\mathrm{p}_{1/2}$) and sea quark excitations ($n\bar{\mathrm{s}}_{1/2}$) cancel exactly, i.e. the model fails to reproduce the convection current terms $O(\mu)$ in the amplitudes $A^{(0,+)}$. The origin of this failure may be traced to the wrong treatment of CM motion in relativistic bag models ('the wrong degrees of freedom moving at the right speed'). If we introduce effective charges for the positive energy contributions and a boost operator for the bag states, the situation may be improved and a qualitative agreement with LET is obtained.

A more quantitative and microscopical treatment has been given by Konen and Drechsel (1991a). Based on a boost for individual quarks bound in a scalar potential, the authors have developed a projection technique to eliminate spurious CM motion from the excitation spectrum. Recoil corrections are treated with the same boost operator. While the static bag model fails completely to reproduce the amplitudes $A^{(0,+)}$, the proposed projection mechanism yields $A^{(0)} = -0.41 \, \mu$ and $A^{(+)} = -0.49 \, \mu$ in close agreement with the LET prediction $A^{(0,+)} = -\tfrac{1}{2} \, \mu$. In particular, this calculation shows that the overlap between a moving ground state and the dipole states ($n\mathrm{p}_{1/2}$) is at least one order of magnitude larger than in the case of the corresponding sea quark state ($n\bar{\mathrm{s}}_{1/2}$). This gives a justification for introducing effective charges for positive but not for negative energy contributions.

In spite of the success of the non-relativistic quark models on one side and the considerable effort necessary to remove spuriosities from relativistic bag models, it is well known that the quarks inside the nucleon move at high velocity. Therefore, it remains an important goal to develop a truly covariant model of the composite

nucleon. As has been recently proposed by Cao and Kisslinger (1990), the most promising formalism for such a task is the light-cone representation allowing for a proper decoupling of CM motion and the internal degrees of freedom and also for a consistent boost of the three-quark system. This light-cone boost also includes the Wigner rotation of the quarks' spin neglected in most 'relativistic' quark models. For a review of this formalism see Lepage and Brodsky (1980) and Namyslowski (1984).

Though the numerical results are somewhat disputed (Drechsel and Weber 1990), the light-cone approach has the interesting feature that the role of the Z-graphs in ordinary perturbation theory is taken over by the instantaneous graph. This contribution can be easily evaluated as an integral over the internal momentum distribution of the quarks in the nucleon. As can be analytically shown, the instantaneous term exactly approaches the Z-graph contribution of table 6 in the limit of large quark masses (Konen and Drechsel 1991b). However, a consistent calculation of the resonance contributions is still missing. While the light-cone approach guarantees the proper covariant behaviour of the wave functions, it does not provide the complete spectrum of intermediate states necessary for calculations. First attempts to construct the dipole excitations of the nucleon have been promising (Konen and Weber 1990). However, they also emphasise the inherent and still unsolved problems of the relativistic many-body system.

5.4. Skyrme model

The Skyrme model (Skyrme 1961) is an effective description of hadronic phenomena at low energies in terms of mesonic degrees of freedom. The renewed interest in this model was motivated by 't Hooft's observation that QCD in the large N_c limit reduces to a theory of weakly interacting pions ('t Hooft 1974) and that baryons may be regarded as solitons in such a theory (Witten 1979). Static properties were calculated in the pioneering work of Adkins *et al* (1983) and were found to agree with experimental values typically at the 30% level. Pion photoproduction in the Skyrme model has been investigated by several authors. The photoproduction of nucleon resonances up to one GeV has been calculated in semiquantitative agreement with experiment (Eckart and Schwesinger 1986, Schwesinger *et al* 1989). Since the model does not contain any parameters specifically adjusted to pion photoproduction, this result is quite encouraging. It has been stressed by Hoodbhoy (1986) that the topological current of the Skyrme model has special consequences for π^0 production.

The Lagrangian of the original Skyrme model is given by

$$\mathcal{L} = \tfrac{1}{4} f_\pi^2 \operatorname{Tr}(\partial_\mu U \, \partial^\mu U^\dagger) + (1/32e^2) \operatorname{Tr}([U^\dagger \, \partial_\mu U, \, U^\dagger \, \partial_\nu U][U^\dagger \, \partial^\mu U, \, U^\dagger \, \partial^\nu U]) \tag{95}$$

where U is an arbitrary $SU(2)$-matrix, f_π the pion decay constant (experimental value $f_\pi \simeq 93$ MeV) and e a parameter determining the size of the soliton. Equation (95) is invariant under global $SU(2) \times SU(2)$ transformations. The corresponding axial (A) and vector (V) Noether currents may be constructed by the variation

$$\delta_A U = -\tfrac{1}{2} \mathrm{i}\{U, \tau\} \qquad \delta_V U = \tfrac{1}{2} \mathrm{i}[U, \tau].$$

If we add a symmetry breaking term to the Lagrangian, e.g.

$$\mathcal{L}_\pi = \tfrac{1}{4} f_\pi^2 m_\pi^2 \operatorname{Tr}(U + U^\dagger - 2) \tag{96}$$

we obtain, to lowest order in the pion field, $U = 1 + i\tau \cdot \pi/f_\pi + [\pi^2]$, the PCAC relation, equation (48).

The construction of a nucleon soliton solution, using the hedgehog ansatz $U_0(x) = \exp(i\tau \cdot \hat{x}F(r))$, and its subsequent quantization is discussed in detail by Holzwarth and Schwesinger (1986). The momentum and kinetic energy of the soliton may be included by replacing x by $s(t) = x - R(t)$ and treating R as a collective coordinate. The electromagnetic current of the Skyrmion contains the third component of the isovector Noether current,

$$J_3^\mu[U] = \tfrac{1}{4} i f_\pi^2 \operatorname{Tr}(\partial^\mu U^\dagger[U, \tau_3]) + (i/16e^2) \operatorname{Tr}([U^\dagger \, \partial_\nu U, U^\dagger[U, \tau_3]][U^\dagger \, \partial^\nu U, U^\dagger \, \partial^\mu U])$$

(97)

and as isoscalar part the anomalous topological current

$$J_0^\mu[U] = (1/48\pi^2)\varepsilon_{\mu\nu\rho\sigma} \operatorname{Tr}(U^\dagger \, \partial^\nu U U^\dagger \, \partial^\rho U U^\dagger \, \partial^\sigma U).$$

(98)

The pion is coupled to the nucleon soliton solution in two different approaches. The first one regards the pion as small amplitude fluctuation (Eckart and Schwesinger 1986), in the second one the pion is introduced as a chiral perturbation (Schnitzer 1985).

Scherer and Drechsel (1991) have studied the predictions of the Skyrme model at threshold. Since a correct determination of the axial coupling constant in the chiral limit is prerequisite to obtain the Kroll–Ruderman term, it is quite unfortunate that the model has a well known problem to come close to the experimental value of this constant. The model fails completely to reproduce the terms linear in the mass ratio μ. This shortcoming is a consequence of the approximations for the pion–nucleon coupling mechanism and, in particular, of the neglect of the Dirac sea in the theory. For obvious reasons the classical hedghog ansatz and the classical projection technique and quantization do not allow for a truly covariant theory. It is interesting, however, that the non-linearities of the model give rise to sizeable anomalous contributions of the seagull type.

6. Corrections to LET

6.1. t-channel contributions

The predictions of LET depend on gauge and Lorentz invariance as well as the assumption of a partially conserved axial current (PCAC), equation (48). Due to the appearance of m_π^2 on the RHS of equation (48), the divergence of the axial current does not influence the lowest order terms of the expansion of the threshold amplitude given in equation (64). However, there will be higher order contributions due to anomalies (Adler 1970), e.g. because of the decay $\pi^0 \to 2\gamma$ (photon exchange in figure 12(g)) with the divergence

$$D_{\text{anom}}^{(\alpha)} = \delta_{\alpha 3} \frac{e^2}{32\pi^2} \varepsilon_{\mu\nu\rho\sigma} F^{\mu\nu} F^{\rho\sigma}$$

(99)

where ε is an antisymmetrical tensor and F the electromagnetic field tensor. This anomaly gives a contribution of 'leading order' for the production of neutral pions. However, its numerical value is only of the order of 1%. Larger contributions arise if the exchanged photon is replaced by vector mesons. The exchange of ω mesons in

Table 7. Contributions of t-channel vector mesons and s- and u-channel nucleon resonances in the phenomenological model.

	ω	ρ	$\Delta(1232)$	$N^*(1535)$	$\Delta(1620)$	$N^*(1650)$
$\gamma p \to \pi^+ n$	—	0.14	−0.10	1.61	−0.21	0.80
$\gamma n \to \pi^- p$	—	0.14	+0.10	−1.61	0.21	−0.66
$\gamma p \to \pi^0 p$	0.26	0.10	−0.15	0.27	0.06	0.15
$\gamma n \to \pi^0 n$	0.26	−0.10	−0.15	0.27	0.06	0.05

the t-channel decreases the amplitude for $\gamma + p \to \pi^0 + p$ by about 10%, the ρ meson leads to a further reduction by about 3% (see table 7). Clearly, contributions of higher mesons cannot be excluded, but there is no indication for such effects at present.

Using an exchange mechanism as in figure 12(g), with a structureless proton in the intermediate triangle, we obtain the following lowest order terms beyond the LET value of equation (64):

$$A^{(-)} = \left(1 + \frac{g_A^2}{4\pi}\frac{8}{3\pi}\frac{m_\pi^2}{m_A^2 + m_\pi^2}\right) \tag{100}$$

$$A^{(+,0)} = \left(-\tfrac{1}{2}\mu + \tfrac{1}{2}\mu^{(v,s)}\mu^2 + \frac{e^2}{4\pi}\mu^{(s,v)}\frac{\mu}{\pi} + \frac{g_v(g_v + f_v)}{4\pi}\frac{m_\pi^2}{m_v^2 + m_\pi^2}\frac{\mu}{\pi} + \frac{g_T^2}{4\pi}\frac{m_\pi^2}{m_T^2 + m_\pi^2}\frac{16\mu}{3\pi}\right).$$

In these equations, g_A and m_A are coupling constants and masses, respectively, of axial vector–isovector mesons contributing to $E_{0+}^{(-)}$. Similarly V and T refer to vector and tensor mesons, of isoscalar and isovector nature, appearing in $E_{0+}^{(+)}$ and $E_{0+}^{(0)}$, respectively. The constant f_v describes the induced tensor coupling appearing, e.g., for the ρNN vertex. It is interesting to note that all higher order t-channel corrections are positive.

6.2. s- and u-channel contributions and nucleon resonances

Further contributions of higher order in μ are due to intermediate Δ and higher resonances in the s- and u-channels (figure 12(e) and (f)). There have been many calculations investigating the influence of the Δ. Unfortunately, the off-shell extrapolation of propagators and vertices gives rise to large model dependencies. In the standard units of $10^{-3}/m_\pi$, Nath and Singh (1989) find for the Δ contribution $0.34 \geqslant \delta E_{0+}^{(+)} \geqslant -0.10$ and, for the same parameters, $-1.09 \leqslant \delta E_{0+}^{(-)} \leqslant +0.90$. Their theoretically preferred values are 0.10 and −0.02, respectively. Previous estimates of Peccei (1969) and Olsson and Osypowski (1975) have been −0.04. The constituent quark model (CQM) gives the analytical results

$$A_\Delta^{(-)} = -\tfrac{4}{25}\mu_v\mu^2 m_\pi(m_\Delta - m + m_\pi)^{-1} \qquad A_\Delta^{(+)} = 2A_\Delta^{(-)}. \tag{101}$$

Due to the hyperfine interaction $A_\Delta^{(+)}$ is $O(\mu^3)$, as is required by LET. These theorems tacitly assume a non-degenerate ground state. In the limit of a vanishing mass splitting, $m_\Delta \to m$, the Δ contributions would be $O(\mu^2)$!

As far as higher resonances are concerned, we are not aware of any quantitative estimate of their influence on the E_{0+} threshold amplitude. In a phenomenological model the electromagnetic and strong vertices for the transition to N^* resonances should be constructed such that gauge invariance and PCAC are fulfilled. In this way

these resonances may contribute only to higher order, say $O(\mu^3)$ for neutral pion photoproduction, such that the results of LET remain unchanged.

In the case of the CQM, however, the internal degrees of freedom are described explicitly. As a result the contributions of intermediate anti-nucleon states (Z-graphs at the nucleon level) are replaced by intermediate anti-quark states (sea quark contributions) and valence quark excitations (dipole states). Therefore, these dipole states are essential to obtain the result of LET in the CQM and only the terms beyond LET should be counted as additional model-dependent contributions. As is well known from the work of Copley *et al* (1969), both convection and spin currents contribute to photoexcitation, leading to an exact cancellation for the $A_{1/2}$ amplitude of the N*(1688) for $\omega^2 = 2\alpha_0^2$, for an oscillator parameter $\alpha_0^2 = 0.17$ GeV^2. With harmonic oscillator wave functions, only the dipole states $S_{11}(1535)$, $S_{11}(1650)$ and $S_{31}(1620)$ can contribute beyond the nucleon and Δ intermediate states. Assuming that these states are degenerate at $\omega_0 = m^* - m = 3\alpha_0^2/m$, their combined contribution is

$$A_{dip}^{(+)} = \tfrac{2}{5}\mu(1 + \tfrac{9}{2}\mu^2 m/\omega_0)/(1 - \mu^2 m^2/\omega_0^2)$$

$$A_{dip}^{(0)} = \mu^3(m/\omega_0)/(1 - \mu^2 m^2/\omega_0^2) \tag{102}$$

$$A_{dip}^{(-)} = \mu^2(m/\omega_0)(1 + \tfrac{6}{5}\mu^2 m/\omega_0)/(1 - \mu^2 m^2/\omega_0^2).$$

The leading term in $A^{(+)}$, $\tfrac{2}{5}\mu$, is due to the convection current and is already contained in LET. All higher terms, of relative order μ^2, are model-dependent terms *beyond* LET. In the usual units of $10^{-3}/m_\pi$, the multipole contributions beyond LET are $\delta E_{0+}^{(+)} = 0.29$, $\delta E_{0+}^{(0)} = 0.11$ and $\delta E_{0+}^{(-)} = 0.82$. As a consequence, $\delta E_{0+}(p\pi^0) = 0.40$ gives a relatively large correction, essentially due to the spin current of the quarks.

The results obtained in the framework of the CQM can only serve as a qualitative guide. They are interesting in so far as they can reproduce LET (for pseudovector pion quark coupling!) and because the estimated total effect of resonance contributions to threshold production of neutral pions on the proton is not larger than about 10%. In the case of phenomenological isobar models the estimates are of the same order of magnitude. Fixing the strong πNN^* coupling to the pion decay width of the resonance and the electromagnetic γNN^* coupling to the radiative decay width, we obtain the contributions shown in table 7. These numbers do not contain antiparticle contributions from nucleon resonances (i.e. intermediate anti-isobar states). The use of off-shell form factors will reduce the contributions of the higher resonances considerably.

6.3. Final state interactions

Due to the suppression of neutral pion production at threshold by a factor μ, the rescattering graph of figure 12(i) may become important (Laget 1981). It involves the production of a positive pion followed by charge exchange. The rapid cross-over from complex to real values of the amplitude might give rise to a cusp effect at threshold ('Wigner cusp'). Since the loop diagram diverges, the results are strongly dependent on form factors and/or renormalization procedures.

Earlier estimates of rescattering were based on an extrapolation of the k-matrix to momenta below the $\pi^+ n$ threshold. The relevant matrix element is related to the imaginary part of the rescattering diagram. Being on-shell, it can be expressed by

the photoproduction of a π^+ followed by the charge exchange scattering $\pi^+ n \rightarrow \pi^0 p$. While the photoproduction of charged pions is much more likely than that one of neutral pions, the process is reduced by the smallness of the scattering length for charge exchange near threshold,

$$E_{0+} = E_{0+}(p\pi^0) + ik_{\pi^+}a(n\pi^+ \rightarrow p\pi^0)E_{0+}(n\pi^+) \tag{103}$$

where k_{π^+} is the momentum of the π^+. Below threshold, the correction is obtained by $k_\pi \rightarrow ik_\pi$, resulting in a real value of the S-wave amplitude. Unfortunately, this correction increases the discrepancy between LET and the data.

Final state interactions have recently been investigated in a dynamical model by Yang (1989), Nozawa *et al* (1990), Lee *et al* (1991), Lee and Pearce (1991) and Bergstrom (1991). In a coupled channels calculation the πN t-matrix is evaluated and form factors of the model are fitted to the πN phase shifts up to about 500 MeV pion laboratory energy (see figure 4).

Using isospin symmetry, i.e. equal masses for neutral and charged pions, the half-off-shell t-matrix is given by

$$t^\alpha(k_0, k, W) = e^{i\delta_\alpha} \cos \delta_\alpha k^\alpha(k_0, k, W)$$

$$k^\alpha(k_0, k, W) = v^\alpha(k_0, k, W) + P \int dk' k'^2 \frac{v^\alpha(k_0, k', W)k^\alpha(k', k, W)}{W - W_{\pi N}(k')} \tag{104}$$

with $\alpha = \{lJI\}$ for angular momentum, spin and isospin, the phase shifts δ_α and the CM energy of the πN system

$$W_{\pi N}(k') = (m^2 + k'^2)^{1/2} + (m_\pi^2 + k'^2)^{1/2}. \tag{105}$$

In different approaches the driving (potential) terms v^α are taken either from separable potentials or from πN Lagrangians. The (real) k-matrix k^α is related to the phase shifts for on-shell values by

$$\tan \delta_\alpha(W) = -\rho(k_0)k^\alpha(k_0, k_0, W) \tag{106}$$

with $\rho(k_0) = \pi k_0 E_\pi(k_0)E_N(k_0)/W$ and $W = W_{\pi N}(k_0)$.

Though all these models reproduce the on-shell phase shifts reasonably well, they differ in the half-off-shell case being probed by photoproduction,

$$t^\alpha_{\gamma\pi}(k_0, q, W) = v^\alpha_{\gamma\pi}(k_0, q, W) + \int dk k^2 \frac{t^\alpha_{\pi N}(k_0, k, W)v^\alpha_{\gamma\pi}(k, q, W)}{W - W_{\pi N}(k) + i\varepsilon}$$

$$= e^{i\delta_\alpha} \cos \delta_\alpha \left\{ v^\alpha_{\gamma\pi}(k_0, q) + P \int dk k^2 \frac{k^\alpha(k_0, k, W)v^\alpha_{\gamma\pi}(k, q, W)}{W - W_{\pi N}(k)} \right\}. \tag{107}$$

In the above expression Watson's final state theorem is exactly fulfilled (Watson 1954)

$$t^\alpha_{\gamma\pi} = \pm e^{i\delta_\alpha} |t^\alpha_{\gamma\pi}|$$

since both the Born terms $v^\alpha_{\gamma\pi}$ and the k-matrix k^α are real functions. Therefore, contributions from the Δ-resonance are contained in $v^\alpha_{\gamma\pi}$ only by its bare (unrenormalized) form without a decay width. In this idealized case without pion mass splitting, equation (107) leads to an E_{0+} amplitude at threshold which should be identical to the result of the LET. Possible deviations can arise from violations of the basic invariances required by the LET. Even if a phenomenological pion–nucleon

potential describes the on-shell πN data it is not clear whether its off-shell continuation is in agreement with PCAC requirements. Similarly, gauge invariance is not automatically guaranteed for off-shell processes.

Without a cut-off (off-shell form factor) in the driving terms for both the πN interaction v^α and the (γ, π) amplitude $v^\alpha_{\gamma,\pi}$, the principal value integral of equation (107) diverges. Therefore the result of such calculations depends strongly on the value of the cut-off mass Λ in the off-shell form factors. As a consequence, the low energy expansion of the amplitudes contains a parameter m_π/Λ in addition to the parameter $\mu = m_\pi/m$ of LET.

The Adler–Dothan (1966) theorem asserts that the higher-order terms, such as rescattering (figure 12(i)), contribute only to a relative order of μ^2. This requires, however, that these higher-order terms have to be calculated in a consistent framework of covariant perturbation theory, while the coupled channels calculations take into account only classes of diagrams.

As an additional problem, the mass difference of $m_{\pi^\pm} - M_{\pi^0} \simeq 4.6\,\text{MeV}$ gives rise to isospin symmetry breaking and drastic changes of E_{0+} at threshold may become possible. For the case of (γ, π^0) on the proton, equation (107) takes the form

$$
t_{\gamma,\pi^0 p}(k_0, q) = \exp(i\delta_{\pi^0 p}) \cos \delta_{\pi^0 p} \Big\{ v_{\gamma\pi^0 p}(k_0, q)
$$
$$
- i\Theta(W - m_\pi - m_{\pi^+}) \rho_{\pi^+}(k_+) v_{\gamma\pi^+}(k_+, q) \bar{k}_{\pi^+ n \to \pi^0 p}(k_0, k_+, W)
$$
$$
+ P \int dk k^2 \frac{\bar{k}_{\pi^0 p \to \pi^0 p}(k_0, k, W) v_{\gamma,\pi^0 p}(k, q)}{W - W_{\pi^0 p}(k)}
$$
$$
+ P \int dk k^2 \frac{\bar{k}_{\pi^+ n \to \pi^0 p}(k_0, k, W) v_{\gamma,\pi^+}(k, q)}{W - W_{\pi^+ n}(k)} \Big\}, \tag{108}
$$

where k_0 and k_+ are the on-shell momenta of π^0 and π^+ respectively, and $\bar{k}$ is defined by the half-off-shell relation

$$
t_{\pi N \to \pi^0 p}(k_0, k, W) = \exp(i\delta_{\pi^0 p}) \cos \delta_{\pi^0 p} \bar{k}_{\pi N \to \pi^0 p}(k_0, k, W). \tag{109}
$$

The three terms in curly brackets on the RHS of equation (108) are:
(i) the Born amplitude for $\gamma p \to \pi^0 p$;
(ii) the imaginary contribution of π^+ production followed by charge exchange scattering, it appears only above the $\pi^+ n$ threshold;
(iii) the contributions of rescattering expressed by the principal value integrals, P.

The simple k-matrix approximation of equation (103), used in the early experimental analyses, is obtained from equation (108) by dropping the principal value integrals, extrapolating the Θ-function part below π^+ threshold, and evaluating equation (106) at threshold, $\tan \delta \to ka$.

The parameters of Nozawa et al (1990) have been fitted to pion–nuclear scattering and pion photoproduction in the Δ region (P-wave amplitudes M_{1+} and E_{1+}). With a reasonable cut-off $\Lambda = 650\,\text{MeV}$ they obtain a good overall agreement with the data at higher energies. In the threshold region the calculation is characterized by strong cancellations of the effects of final state interactions for $\pi^+ n$ and $\pi^0 p$ channels as well as pion pole and Kroll–Ruderman terms (see table 8).

The final result shows that higher order contributions cancel to a large degree. This is also borne out in an analytical calculation by Naus et al (1990). In a consistent expansion of the threshold amplitude about the soft-pion point, the authors precisely obtain LET. All off-shell behaviour of the vertices disappears in the

Table 8. Contributions of Born diagrams and final state interactions to the threshold S-wave amplitude $E_{0+}(\gamma p \to \pi^0 p)$ in units of $10^{-3}/m_\pi$. B, Born terms for the diagrams (a)–(d) of figure 12 and ω/ρ exchange (figure 12(g)). FSI(π^0), corrections for rescattering of π^0. FSI(π^+), production of π^+ followed by charge exchange scattering. Results from Nozawa *et al* (1990).

	(a)	(b)	(c)	(d)	ω/ρ	Sum
B	−1.26	−1.25	0	0	0.22	−2.29
FSI(π^0)	−0.10	0.57	0	0	0.05	0.52
FSI(π^+)	−0.53	−0.24	−3.07	3.57	0.10	−0.15
Sum	−1.89	−0.92	−3.07	3.57	0.37	−1.92

final answer, and rescattering corrections only contribute in higher order terms not specified by LET.

In figure 13 we show the model dependence of rescattering corrections for the reaction $\gamma p \to \pi^0 p$. While all calculations reproduce the πN phase shifts reasonably well, they differ in the off-shell continuations of the k-matrix in equations (107) and (108). As an example, figure 14 shows the half-off-shell matrix elements of two separable and a meson exchange potential used in such calculations. As a consequence the results obtained for the real part of the E_{0+} amplitude differ substantially. The corresponding curves $b_{1,2,3}$ in figure 13 cover a wide range between LET and even positive values for E_{0+}.

The three calculations $b_{1,2,3}$ assume isospin symmetry, equation (107), i.e. the thresholds for neutral and charged pions coincide, resulting in a very smooth energy dependence of the amplitude. A similar behaviour is seen in curve a, except for the region of the γ, π^+ threshold at 151.4 MeV, where, due to the Θ-function in equation (108), a cusp effect occurs. Starting from a chirally invariant Lagrangian, Lee and Pearce (1991) have obtained a much larger rescattering effect, curve c. However, it has not yet been possible to preserve chiral symmetry in the course of the coupled channels calculation.
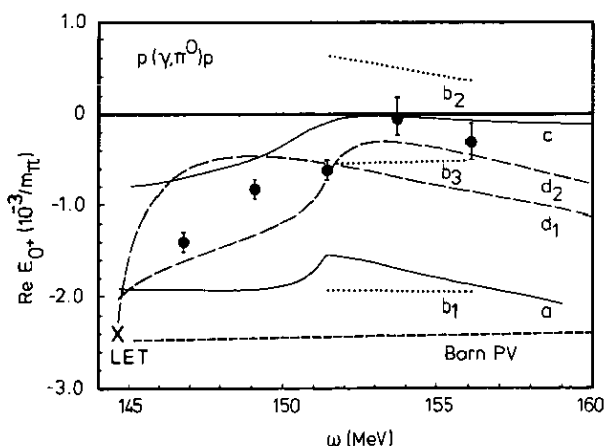

Figure 13. Model dependence of rescattering calculations for Re E_{0+} in the reaction $\gamma p \to \pi^0 p$. a, Nozawa *et al* (1990); $b_{1,2,3}$, Lee *et al* (1991), with two separable potentials and a meson exchange model (b_3) respectively; c, Lee and Pearce (1991); $d_{1,2}$, Bergstrom (1991), with and without isospin symmetry, respectively. For comparison we show the result of the Born terms in pseudovector coupling which is very close to the LET prediction at threshold. Experimental data as in figure 11.
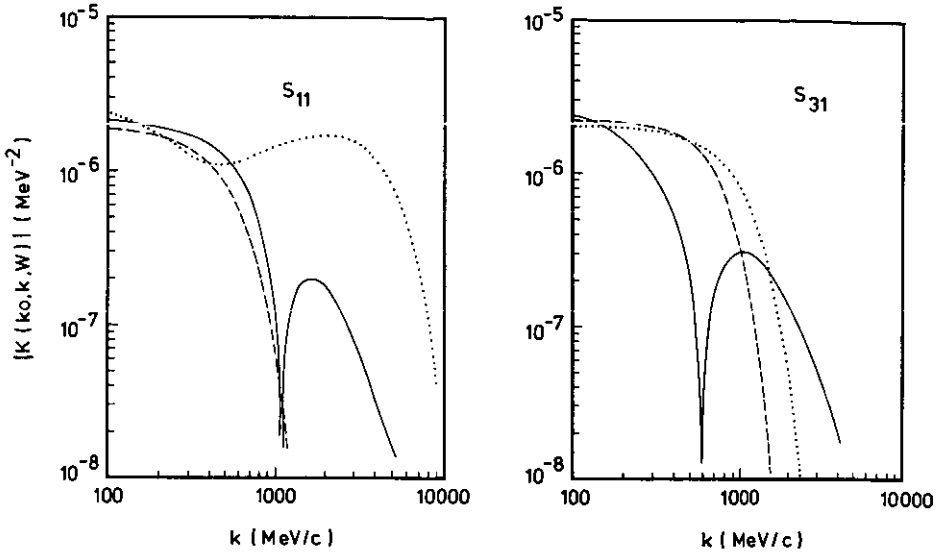
Figure 14. Half-off-shell matrix element of the πN k-matrix for energy 3 MeV above threshold according to Lee *et al* (1991). The dotted, broken and full curves show the results of two separable πN potentials and a meson exchange model, respectively, in the same sequence as curves $b_{1,2,3}$ of figure 13.

A very rapid change in the E_{0+} amplitude shows up in the calculation of Bergstrom (1991), curves $d_{1,2}$. Keeping LET as a constraint for the isospin symmetrical case (d_1), phenomenological off-shell form factors are introduced with rather strong energy dependence in order to fit the data (d_2).

At this point it is evident that the search for fundamental effects like chiral symmetry breaking in threshold pion production or even subnucleonic degrees of freedom (sigma term) become totally obscured by the present model dependence of rescattering effects.

A possible approach avoiding these problems might be a chiral perturbation theory without any additional off-shell parameter. It remains to be seen whether such calculations confirm the expansion of LET or if additional terms such as $\log(m_\pi/m)$ appear†.

7. Summary and conclusions

Investigations with electromagnetic interactions have contributed substantially to our knowledge of the structure of hadrons. With the advent of the new accelerators, polarization degrees of freedom will play a decisive role in unravelling the unsettled questions. Typical examples range from the distribution of the neutron's charge seen in elastic electron scattering to the spin content of the nucleon in deep inelastic scattering and its relation to QCD based predictions.

Photo- and electroexcitation of the nucleon and meson production promise to determine some of the most wanted observables at intermediate energies, e.g.

---

† In a very recent paper by Bernard *et al* (1991) the threshold amplitude for neutral pion photoproduction has been studied to one loop in chiral perturbation theory. In a certain class of diagrams there appear logarithmic singularities violating the usual assumption of LET that the amplitude can be expanded around the soft-pion point. As a consequence they obtain additional large terms of order μ^2

(i) the L_{1+}/E_{1+} amplitude in the range of the $\Delta(1232)$ related to the intrinsic deformation of the nucleon,
(ii) the L_{1-} amplitude, particularly for the Roper $N^*(1440)$, the breathing mode of the nucleon,
(iii) the high rate for η meson production near the $N^*(1535)$ and at higher energies,
(iv) the production of two pions or more in order to test consequences of chiral symmetry and the interaction of low energy pions or to find the 'missing resonances' at higher energy.

The strange behaviour of the threshold E_{0+} amplitude has added another challenge to future experiments. As may be seen in figure 15, the Mainz results show an amplitude dropping from its LET value at π^0 threshold to essentially zero at π^+ threshold, while the existing multipole analyses of the data at the higher energies predict a slowly varying function with a mean value close to LET. Both the fluctuation at small energies and the large statistical and systematical error bars at the higher energies show the need for new and vigorous investigations in order to bridge the gap between the new and the old data. This includes the challenge to measure $n(\gamma, \pi^0)n$ together with $p(\gamma, \pi^0)p$ in 'quasifree kinematics' for ^2H and ^3H targets, because the fourth physical amplitude allows violations of isospin symmetry to be studied. Of similar interest is the study of the $(e, e'\pi^0)$ reaction in order to see whether the threshold puzzle persists for the L_{0+} amplitude and, at the higher momenta, to check the consistency of the models and the influence of the nucleon's axial and vector form factors and of the pion form factor on the production mechanism.

With the Mainz Microtron the first accelerator of a new generation has gone into operation to meet the challenge of the experiments proposed above. The high-duty factor and the high current of these accelerators will be a prerequisite for crossing the new frontier in electromagnetic physics, the transition from inclusive(single-arm)
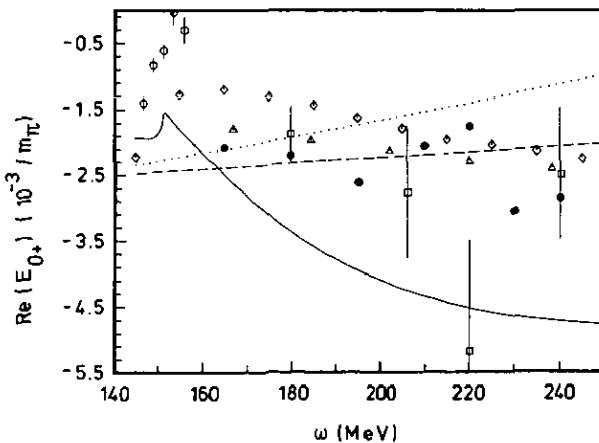

Figure 15. Real part of the E_{0+} amplitude for the reaction $\gamma p \to \pi^0 p$ between threshold and 250 MeV photon energy. Broken curve, Born terms with PV coupling; dotted curve, Born terms plus vector meson exchange and Δ contribution, full curve rescattering calculations (Nozawa *et al* 1990, Blankleider 1991). The data points refer to the following multipole analyses: $\oplus$, Mainz data (as in caption to table 5); $\square$, Pfeil and Schwela (1972); $\bullet$, Berends and Donnachie (1975); $\triangle$, Crawford and Morton (1983); $\diamondsuit$, Arndt *et al* (1990).

to coincidence experiments. This development will allow study of the correlations between the constituents of the nucleon in a qualitatively novel way, at a time when the problem of strong interactions in the confinement phase becomes ever more interesting. Such investigations require a high degree of precision and endeavour. However, they will increase our knowledge of the hadronic structure in a qualitative way, contribute to a better understanding of the confinement problem and, very likely, will lead to the discovery of new exciting phenomena.

Appendix A. Transformation of differential cross section

The laboratory cross section can be easily obtained by multiplying equation (22) with the Jacobian

$$\frac{d\Omega_\pi^{CM}}{d\Omega_\pi^L} = \frac{|k|^2 W}{|k_{CM}|\,|(m_i + \omega)|\,k\,|-\omega_\pi|\,q\,|\cos\Theta_\pi|}$$

where all variables (except k_{CM}) are evaluated in the laboratory frame. The angular distribution for the recoiling nucleon may be obtained using the Jacobian

$$\frac{d\Omega_\pi^{CM}}{d\Omega_N^L} = \frac{|P_f|^2 W}{|k_{CM}|\,|(m_i + \omega)|\,P_f\,|-E_f|\,q\,|\cos\Theta_N|}.$$

Appendix B. The response functions for photo- and electroproduction including target and recoil polarization

In this appendix we express the response functions of equation (27) in terms of the CGLN amplitudes of equation (4). All angles are pion CM angles, i.e. $\Theta = \Theta_\pi$, $\Phi = \Phi_\pi$. Both the polarization of the target and of the recoiling nucleon are measured with regard to the three axes $\hat{l}$ (along the momentum of the outgoing nucleon), $\hat{t} \approx \hat{n} \times \hat{l}$ and $\hat{n}$ (normal to the reaction plane, in the direction of $\hat{q} \times \hat{k}$). For example, $P_n = \hat{n} \cdot \hat{S}_R$ is the projection of the spin vector (in the proton rest frame!) unto the axis normal to the reaction plane.

In the formulae the subscripts i, f in $l_{i,f}, t_{i,f}$ and $n_{i,f}$ denote target or recoil polarization, respectively.

$$\frac{d\sigma_v}{d\Omega_\pi^{CM}} = \frac{|k|}{k_\gamma^{CM}} \{\tfrac{1}{2}(W_{xx} + W_{yy}) + \varepsilon_L W_{zz} - [2\varepsilon_L(1 + \varepsilon)]^{1/2}\,\text{Re }W_{xz}$$

$$+ \tfrac{1}{2}\varepsilon(W_{xx} - W_{yy}) + h[2\varepsilon_L(1 - \varepsilon)]^{1/2}\,\text{Im }W_{yz} + h(1 - \varepsilon^2)^{1/2}\,\text{Im }W_{xy}\}$$

with the transverse response functions

$$\tfrac{1}{2}(W_{xx} + W_{yy}) = R_T + P_n R_T(n)$$

$$R_T = |F_1|^2 + |F_2|^2 + \tfrac{1}{2}\sin^2\Theta(|F_3|^2 + |F_4|^2)$$

$$- \text{Re}\{2\cos\Theta F_1^* F_2 - \sin^2\Theta(F_1^* F_4 + F_2^* F_3 + \cos\Theta F_3^* F_4)\}$$

$$R_T(n_i) = +\sin\Theta\,\text{Im}\{F_1^* F_3 - F_2^* F_4 + \cos\Theta(F_1^* F_4 - F_2^* F_3) - \sin^2\Theta F_3^* F_4\}$$

$$R_T(n_f) = -\sin\Theta\,\text{Im}\{2F_1^* F_2 + F_1^* F_3 - F_2^* F_4 + \cos\Theta(F_1^* F_4 - F_2^* F_3) - \sin^2\Theta F_3^* F_4\}$$

$$R_T(l) = R_T(t) = 0$$

the longitudinal response functions

$$W_{zz} = R_L + P_n R_L(n)$$

$$R_L = |F_5|^2 + |F_6|^2 + 2\cos\Theta\,\mathrm{Re}\{F_5^* F_6\}$$

$$R_L(n_i) = -R_L(n_f) = -2\sin\Theta\,\mathrm{Im}\{F_5^* F_6\}$$

$$R_L(l) = R_L(t) = 0$$

the response functions for transverse–longitudinal interferences

$$\mathrm{Re}\,W_{xz} = -\cos\Phi R_{TL} - \sin\Phi P_l R_{TL}(l) - \sin\Phi P_t R_{TL}(t) - \cos\Phi P_n R_{TL}(n)$$

$$R_{TL} = -\sin\Theta\,\mathrm{Re}\{(F_2^* + F_3^* + \cos\Theta F_4^*)F_5 + (F_1^* + F_4^* + \cos\Theta F_3^*)F_6\}$$

$$R_{TL}(l_i) = \sin\Theta\,\mathrm{Im}\{F_1^* - 2\cos\Theta F_2^*)F_5 - F_2^* F_6\}$$

$$R_{TL}(l_f) = -\sin\Theta\,\mathrm{Im}\{F_1^* F_5 + F_2^* F_6\}$$

$$R_{TL}(t_i) = \mathrm{Im}\{(\cos\Theta F_1^* - \cos 2\Theta F_2^*)F_5 + (F_1^* - \cos\Theta F_2^*)F_6\}$$

$$R_{TL}(t_f) = \mathrm{Im}\{(F_2^* - \cos\Theta F_1^*)F_5 - (F_1^* - \cos\Theta F_2^*)F_6\}$$

$$R_{TL}(n_i) = -R_{TL}(n_f) = -\mathrm{Im}\{(F_1^* - \cos\Theta F_2^* + \sin^2\Theta F_4^*)F_5$$
$$- (F_2^* - \cos\Theta F_1^* + \sin^2\Theta F_3^*)F_6\}$$

the response functions for transverse–transverse interferences

$$\tfrac{1}{2}(W_{xx} - W_{yy}) = \cos 2\Phi R_{TT} + \sin 2\Phi P_l R_{TT}(l) + \sin 2\Phi P_t R_{TT}(t) + \cos 2\Phi P_n R_{TT}(n)$$

$$R_{TT} = +\sin^2\Theta(\tfrac{1}{2}(|F_3|^2 + |F_4|^2) + \mathrm{Re}\{F_1^* F_4 + F_2^* F_3 + \cos\Theta F_3^* F_4\})$$

$$R_{TT}(l_i) = -\sin^2\Theta\,\mathrm{Im}\{2F_1^* F_2 + F_1^* F_3 - F_2^* F_4 - 2\cos\Theta F_2^* F_3\}$$

$$R_{TT}(l_f) = +\sin^2\Theta\,\mathrm{Im}\{F_1^* F_3 + F_2^* F_4\}$$

$$R_{TT}(t_i) = -\sin\Theta\,\mathrm{Im}\{F_1^* F_4 + \cos\Theta(2F_1^* F_2 + F_1^* F_3 - F_2^* F_4) - \cos 2\Theta F_2^* F_3\}$$

$$R_{TT}(t_f) = \sin\Theta\,\mathrm{Im}\{F_1^* F_4 - F_2^* F_3 + (F_1^* F_3 - F_2^* F_4)\cos\Theta\}$$

$$R_{TT}(n_i) = +\sin\Theta\,\mathrm{Im}\{2F_1^* F_2 + F_1^* F_3 - F_2^* F_4 + \cos\Theta(F_1^* F_4 - F_2^* F_3) - \sin^2\Theta F_3^* F_4\}$$

$$R_{TT}(n_f) = -\sin\Theta\,\mathrm{Im}\{F_1^* F_3 - F_2^* F_4 + (F_1^* F_4 - F_2^* F_3)\cos\Theta - F_3^* F_4 \sin^2\Theta\}$$

the response functions for polarized electrons and transverse–longitudinal interferences

$$\mathrm{Im}\,W_{yz} = \sin\Phi R_{TL'} + \cos\Phi P_l R_{TL'}(l) + \cos\Phi P_t R_{TL'}(t) + \sin\Phi P_n R_{TL'}(n)$$

$$R_{TL'} = -\sin\Theta\,\mathrm{Im}\{(F_2^* + F_3^* + \cos\Theta F_4^*)F_5 + (F_1^* + F_4^* + \cos\Theta F_3^*)F_6\}$$

$$R_{TL'}(l_i) = \sin\Theta\,\mathrm{Re}\{(F_1^* - 2\cos\Theta F_2^*)F_5 - F_2^* F_6\}$$

$$R_{TL'}(l_f) = -\sin\Theta\,\mathrm{Re}\{F_1^* F_5 + F_2^* F_6\}$$

$$R_{TL'}(t_i) = \mathrm{Re}\{(\cos\Theta F_1^* - \cos 2\Theta F_2^*)F_5 + (F_1^* - \cos\Theta F_2^*)F_6\}$$

$$R_{TL'}(t_f) = \mathrm{Re}\{(F_2^* - \cos\Theta F_1^*)F_5 - (F_1^* - \cos\Theta F_2^*)F_6\}$$

$$R_{TL'}(n_i) = -R_{TL'}(n_f) = \mathrm{Re}\{(F_1^* - \cos\Theta F_2^* + \sin^2\Theta F_4^*)F_5$$
$$- (F_2^* - \cos\Theta F_1^* + \sin^2\Theta F_3^*)F_6\}$$

and the response functions for polarised electrons and transverse–transverse interferences

$$\text{Im } W_{xy} = P_l R_{TT'}(l) + P_t R_{TT'}(t)$$

$$R_{TT'}(l_i) = \cos\Theta(|F_1|^2 + |F_2|^2)$$
$$\qquad - \text{Re}\{2\cos^2\Theta F_1^* F_2 + \sin^2\Theta(F_1^* F_3 - F_2^* F_4 - 2\cos\Theta F_2^* F_3)\}$$

$$R_{TT'}(l_f) = -\cos\Theta(|F_1|^2 + |F_2|^2) + \text{Re}\{2F_1^* F_2 + \sin^2\Theta(F_1^* F_3 + F_2^* F_4)\}$$

$$R_{TT'}(t_i) = -\sin\Theta(|F_1|^2 + |F_2|^2 + \text{Re}\{F_1^* F_4 - \cos\Theta(2F_1^* F_2$$
$$\qquad - F_1^* F_3 + F_2^* F_4) - \cos 2\Theta F_2^* F_3\})$$

$$R_{TT'}(t_f) = \sin\Theta(|F_1|^2 - |F_2|^2 + \text{Re}\{F_1^* F_4 - F_2^* F_3 + \cos\Theta(F_1^* F_3 - F_2^* F_4)\})$$

$$R_{TT'}(n) = 0.$$

Appendix C. Multipole decompositions of the response functions

Using the multipole decomposition of the CGLN amplitudes of equation (8), the structure functions are expressed in multipoles up to $l = 1$.

$$R_T = |E_{0+}|^2 + \tfrac{1}{2}|2M_{1+} + M_{1-}|^2 + \tfrac{1}{2}|3E_{1+} - M_{1+} + M_{1-}|^2$$
$$\qquad + 2\cos\Theta\,\text{Re}\{E_{0+}^*(3E_{1+} + M_{1+} - M_{1-})\}$$
$$\qquad + \cos^2\Theta(|3E_{1+} + M_{1+} - M_{1-}|^2 - \tfrac{1}{2}|2M_{1+} + M_{1-}|^2$$
$$\qquad - \tfrac{1}{2}|3E_{1+} - M_{1+} + M_{1-}|^2)$$

$$R_T(n_i) = 3\sin\Theta\,\text{Im}\{E_{0+}^*(E_{1+} - M_{1+}) - \cos\Theta(E_{1+}^*(4M_{1+} - M_{1-}) + M_{1+}^* M_{1-})\}$$

$$R_T(n_f) = -\sin\Theta\,\text{Im}\{E_{0+}^*(3E_{1+} + M_{1+} + 2M_{1-}) + 3\cos\Theta(3E_{1+}^* + M_{1+}^*)M_{1-}\}$$

$$R_L = |L_{0+}|^2 + 4|L_{1+}|^2 + |L_{1-}|^2 - 4\text{Re}\{L_{1+}^* L_{1-}\}$$
$$\qquad + 2\cos\Theta\,\text{Re}\{L_{0+}^*(4L_{1+} + L_{1-})\} + 12\cos^2\Theta(|L_{1+}|^2 + \text{Re}\{L_{1+}^* L_{1-}\})$$

$$R_L(n_i) = -R_L(n_f) = +2\sin\Theta\,\text{Im}\{L_{0+}^*(2L_{1+} - L_{1-}) - 6\cos\Theta L_{1+}^* L_{1-}\}$$

$$R_{TL} = -\sin\Theta\,\text{Re}\{L_{0+}^*(3E_{1+} - M_{1+} + M_{1-}) - (2L_{1+}^* - L_{1-}^*)E_{0+}$$
$$\qquad + 6\cos\Theta(L_{1+}^*(E_{1+} - M_{1+} + M_{1-}) + L_{1-}^* E_{1+})\}$$

$$R_{TL}(l_i) = -\sin\Theta\,\text{Im}\{L_{0+}^* E_{0+} + (2L_{1+}^* - L_{1-}^*)(2M_{1+} + M_{1-})$$
$$\qquad + \cos\Theta(L_{0+}^*(3E_{1+} - M_{1+} - 2M_{1-}) + 6L_{1+}^* E_{0+})$$
$$\qquad + 6\cos^2\Theta L_{1+}^*(3E_{1+} - M_{1+} - 2M_{1-})\}$$

$$R_{TL}(l_f) = \sin\Theta\,\text{Im}\{L_{0+}^* E_{0+} - (2L_{1+}^* - L_{1-}^*)(2M_{1+} + M_{1-})$$
$$\qquad + 3\cos\Theta(L_{0+}^*(E_{1+} + M_{1+}) + 2L_{1+}^* E_{0+}) + 18\cos^2\Theta L_{1+}^*(E_{1+} + M_{1+})\}$$

$$R_{TL}(t_i) = -\text{Im}\{L_{0+}^*(2M_{1+} + M_{1-}) - (2L_{1+}^* - L_{1-}^*)E_{0+}$$
$$\qquad + \cos\Theta(L_{0+}^* E_{0+} - 2L_{1+}^*(3E_{1+} - 5M_{1+} - 4M_{1-})$$
$$\qquad + L_{1-}^*(3E_{1+} + M_{1+} - M_{1-})) + \cos^2\Theta(L_{0+}^*(3E_{1+} - M_{1+} - 2M_{1-})$$
$$\qquad + 6L_{1+}^* E_{0+}) + 6\cos^3\Theta L_{1+}^*(3E_{1+} - M_{1+} - 2M_{1-})\}$$

$$R_{TL}(t_f) = -\text{Im}\{L_{0+}^*(2M_{1+} + M_{1-}) + (2L_{1+}^* - L_{1-}^*)E_{0+}$$
$$-\cos\Theta(L_{0+}^*E_{0+} - 2L_{1+}^*(3E_{1+} + 7M_{1+} + 2M_{1-})$$
$$+ L_{1-}^*(3E_{1+} + M_{1+} - M_{1-}))$$
$$-3\cos^2\Theta(L_{0+}^*(E_{1+} + M_{1+}) + 2L_{1+}^*E_{0+}) - 18\cos^3\Theta L_{1+}^*(E_{1+} + M_{1+})\}$$

$$R_{TL}(n_i) = -R_{TL}(n_f) = \text{Im}\{L_{0+}^*E_{0+} + (2L_{1+}^* - L_{1-}^*)(3E_{1+} - M_{1+} + M_{1-})$$
$$+ \cos\Theta(L_{0+}^*(3E_{1+} + M_{1+} - M_{1-}) + (4L_{1+}^* + L_{1-}^*)E_{0+})$$
$$+ 6\cos^2\Theta(L_{1+}^*(E_{1+} + M_{1+} - M_{1-}) + L_{1-}^*E_{1+})\}$$

$$R_{TT} = 3\sin^2\Theta(\tfrac{3}{2}|E_{1+}|^2 - \tfrac{1}{2}|M_{1+}|^2 - \text{Re}\{E_{1+}^*(M_{1+} - M_{1-}) + M_{1+}^*M_{1-}\})$$

$$R_{TT}(l_i) = -\sin^2\Theta\,\text{Im}\{E_{0+}^*(3E_{1+} + M_{1+} + 2M_{1-}) + 6\cos\Theta E_{1+}^*(M_{1+} + 2M_{1-})\}$$

$$R_{TT}(l_f) = 3\sin^2\Theta\,\text{Im}\{E_{0+}^*(E_{1+} - M_{1+}) - 6\cos\Theta E_{1+}^*M_{1+}\}$$

$$R_{TT}(t_i) = -\sin\Theta\,\text{Im}\{-3E_{1+}^*(2M_{1+} + M_{1-}) + 3M_{1+}^*M_{1-}$$
$$+ \cos\Theta E_{0+}^*(3E_{1+} + M_{1+} + 2M_{1-}) + 6\cos^2\Theta E_{1+}^*(M_{1+} + 2M_{1-})\}$$

$$R_{TT}(t_f) = 3\sin\Theta\,\text{Im}\{E_{1+}^*(2M_{1+} + M_{1-}) - M_{1+}^*M_{1-}$$
$$+ \cos\Theta\, E_{0+}^*(E_{1+} - M_{1+}) - 6\cos^2\Theta E_{1+}^*M_{1+}\}$$

$$R_{TT}(n_i) = \sin\Theta\,\text{Im}\{E_{0+}^*(3E_{1+} + M_{1+} + 2M_{1-}) + 3\cos\Theta(3E_{1+}^* + M_{1+}^*)M_{1-}\}$$

$$R_{TT}(n_f) = -3\sin\Theta\,\text{Im}\{E_{0+}^*(E_{1+} - M_{1+}) - \cos\Theta(E_{1+}^*(4M_{1+} - M_{1-}) + M_{1+}^*M_{1-})\}$$

$$R_{TL'} = \sin\Theta\,\text{Im}\{L_{0+}^*(3E_{1+} - M_{1+} + M_{1-}) - (2L_{1+}^* - L_{1-}^*)E_{0+}$$
$$+ 6\cos\Theta(L_{1+}^*(E_{1+} - M_{1+} + M_{1-}) + L_{1-}^*E_{1+})\}$$

$$R_{TL'}(l_i) = \sin\Theta\,\text{Re}\{L_{0+}^*E_{0+} + (2L_{1+}^* - L_{1-}^*)(2M_{1+} + M_{1-})$$
$$+ \cos\Theta(L_{0+}^*(3E_{1+} - M_{1+} - 2M_{1-}^{\cdot}) + 6L_{1+}^*E_{0+})$$
$$+ 6\cos^2\Theta L_{1+}^*(3E_{1+} - M_{1+} - 2M_{1-})\}$$

$$R_{TL'}(l_f) = -\sin\Theta\,\text{Re}\{L_{0+}^*E_{0+} - (2L_{1+}^* - L_{1-}^*)(2M_{1+} + M_{1-})$$
$$+ 3\cos\Theta(L_{0+}^*(E_{1+} + M_{1+}) + 2L_{1+}^*E_{0+}) + 18\cos^2\Theta L_{1+}^*(E_{1+} + M_{1+})\}$$

$$R_{TL'}(t_i) = \text{Re}\{L_{0+}^*(2M_{1+} + M_{1-}) - (2L_{1+}^* - L_{1-}^*)E_{0+}$$
$$+ \cos\Theta(L_{0+}^*E_{0+} - 2L_{1+}^*(3E_{1+} - 5M_{1+} - 4M_{1-})$$
$$+ L_{1-}^*(3E_{1+} + M_{1+} - M_{1-}))$$
$$+ \cos^2\Theta(L_{0+}^*(3E_{1+} - M_{1+} - 2M_{1-}) + 6L_{1+}^*E_{0+})$$
$$+ 6\cos^3\Theta L_{1+}^*(3E_{1+} - M_{1+} - 2M_{1-})\}$$

$$R_{TL'}(t_f) = \text{Re}\{L_{0+}^*(2M_{1+} + M_{1-}) + (2L_{1+}^* - L_{1-}^*)E_{0+}$$
$$- \cos\Theta(L_{0+}^*E_{0+} - 2L_{1+}^*(3E_{1+} + 7M_{1+} + 2M_{1-})$$
$$+ L_{1-}^*(3E_{1+} + M_{1+} - M_{1-}))$$
$$- 3\cos^2\Theta(L_{0+}^*(E_{1+} + M_{1+}) + 2L_{1+}^*E_{0+}) - 18\cos^3\Theta L_{1+}^*(E_{1+} + M_{1+})\}$$

$$R_{TL'}(n_i) = -R_{TL'}(n_f) = -\text{Re}\{L_{0+}^* E_{0+} + (2L_{1+}^* - L_{1-}^*)(3E_{1+} - M_{1+} + M_{1-})$$
$$+ \cos\Theta(L_{0+}^*(3E_{1+} + M_{1+} - M_{1-}) + (4L_{1+}^* + L_{1-}^*)E_{0+})$$
$$+ 6\cos^2\Theta(L_{1+}^*(E_{1+} + M_{1+} - M_{1-}) + L_{1-}^* E_{1+})\}$$

$$R_{TT'}(l_i) = -3\,\text{Re}\{E_{0+}^*(E_{1+} - M_{1+})\}$$
$$+ \cos\Theta(|E_{0+}|^2 - 9\,|E_{1+}|^2 + |M_{1+}|^2 + |M_{1-}|^2$$
$$+ 2\,\text{Re}\{3E_{1+}^*(2M_{1+} + M_{1-}) - M_{1+}^* M_{1-}\})$$
$$+ \cos^2\Theta\,\text{Re}\{E_{0+}^*(9E_{1+} - M_{1+} - 2M_{1-})\}$$
$$+ 6\cos^3\Theta(3\,|E_{1+}|^2 - \text{Re}\{E_{1+}^*(M_{1+} + 2M_{1-})\})$$

$$R_{TT'}(l_f) = \text{Re}\{E_{0+}^*(3E_{1+} + M_{1+} + 2M_{1-})\}$$
$$- \cos\Theta(|E_{0+}|^2 - 9\,|E_{1+}|^2 + |M_{1+}|^2 + |M_{1-}|^2$$
$$- 2\,\text{Re}\{3E_{1+}^*(2M_{1+} + M_{1-}) + M_{1+}^* M_{1-}\})$$
$$- 3\cos^2\Theta\,\text{Re}\{E_{0+}^*(3E_{1+} + M_{1+})\} - 18\cos^3\Theta(|E_{1+}|^2 + \text{Re}\{E_{1+}^* M_{1+}\})$$

$$R_{TT'}(t_i) = -\sin\Theta(|E_{0+}|^2 - 2\,|M_{1+}|^2 + |M_{1-}|^2 + \text{Re}\{3E_{1+}^*(2M_{1+} + M_{1-}) + M_{1+}^* M_{1-}\}$$
$$+ \cos\Theta\,\text{Re}\{E_{0+}^*(9E_{1+} - M_{1+} - 2M_{1-})\}$$
$$+ 6\cos^2\Theta(3\,|E_{1+}|^2 - \text{Re}\{E_{1+}^*(M_{1+} + 2M_{1-})\}))$$

$$R_{TT'}(t_f) = \sin\Theta(|E_{0+}|^2 + 2\,|M_{1+}|^2 - |M_{1-}|^2 - \text{Re}\{3E_{1+}^*(2M_{1+} + M_{1-}) + M_{1+}^* M_{1-}\}$$
$$+ 3\cos\Theta\,\text{Re}\{E_{0+}^*(3E_{1+} + M_{1+})\} + 18\cos^2\Theta(|E_{1+}|^2 + \text{Re}\{E_{1+}^* M_{1+}\})).$$

Appendix D. Response functions in different coordinate systems

The right-handed coordinate system $\{\hat{e}_x, \hat{e}_y, \hat{e}_z\}$ of equation (16) defines the scattering plane of the electron. The reaction plane is defined by the virtual photon, $\hat{q} = (0, 0, 1)$, and the pion, $\hat{k} = (\sin\Theta\cos\Phi, \sin\Theta\sin\Phi, \cos\Theta)$. In the CM frame $\hat{q} = -\hat{P}_i$ and $\hat{k} = -\hat{P}_f$, hence the vector normal to the reaction plane is $\hat{n} = (\hat{P}_i \times \hat{P}_f)/\sin\Theta = (\hat{q} \times \hat{k})/\sin\Theta$.

In the following we will use two different coordinate systems to describe the polarization degrees of freedom. In order to have easy transformation formulae between the two systems, one axis is always chosen normal to the reaction plane.
System 1. Recoil polarization is usually analysed ('Madison convention') in a coordinate system $\{\hat{e}_i, \hat{e}_n, \hat{e}_l\}$, where $\hat{e}_l = \hat{P}_f = -\hat{k}$ points into the direction of the recoiling proton and $\hat{e}_n = \hat{n}$.
System 2. For target polarization it is more convenient to choose a right-handed coordinate system $\{\hat{e}_1, \hat{e}_2, \hat{e}_3\}$, where $\hat{e}_3 = \hat{q}$ points into the direction of the virtual photon and $\hat{e}_2 = \hat{n}$.

The response functions of equation (27) may be written as follows:

$$R_T = \tfrac{1}{2}(|a_0|^2 + |a_t|^2 + |a_n|^2 + |a_l|^2) \qquad R_T(n) = -\text{Im}(a_0 a_n^* \pm a_l a_t^*)$$

$$R_T(l) = R_T(t) = 0 \qquad R_L(l) = R_L(t) = 0$$

$$R_L = |b_l|^2 + |b_t|^2 \qquad R_L(n) = \pm 2\,\text{Im}(b_t b_l^*)$$

Table A1.

$\{\hat{e}_t, \hat{e}_n, \hat{e}_l\}$	$\{\hat{e}_1, \hat{e}_2, \hat{e}_3\}$
$a_0 \approx \sin \Theta F_2$	$a_0 = \sin \Theta F_2$
$a_t = -\cos \Theta F_1 + F_2 + \sin^2 \Theta F_3$	$a_1 = F_1 - \cos \Theta F_2 + \sin^2 \Theta F_4$
$a_n = F_1 - \cos \Theta F_2$	$a_2 = F_1 - \cos \Theta F_2$
$a_l = -\sin \Theta (F_1 + \cos \Theta F_3 + F_4)$	$a_3 = \sin \Theta (F_2 + F_3 + \cos \Theta F_4)$
$b_t = \sin \Theta F_5$	$b_1 = \sin \Theta F_6$
$b_l = -\cos \Theta F_5 - F_6$	$b_3 = F_5 + \cos \Theta F_6$

$$R_{TT} = \tfrac{1}{2}(-|a_0|^2 + |a_t|^2 - |a_n|^2 + |a_l|^2) \qquad R_{TT}(n) = \operatorname{Im}(a_0 a_n^* \mp a_l a_t^*)$$

$$R_{TT}(l) = \operatorname{Im}(a_0 a_l^* \pm a_t a_n^*) \qquad R_{TT}(t) = \operatorname{Im}(a_0 a_t^* \pm a_n a_l^*)$$

$$R_{TT'} = R_{TT'}(n) = 0$$

$$R_{TT'}(l) = -\operatorname{Re}(a_0 a_l^* \mp a_t a_n^*) \qquad R_{TT'}(t) = -\operatorname{Re}(a_0 a_t^* \pm a_n a_l^*)$$

$$R_{TL} = -\operatorname{Re}(a_l b_l^* + a_t b_t^*) \qquad R_{TL}(n) = \mp\operatorname{Im}(a_t b_l^* - a_l b_t^*)$$

$$R_{TL}(l) = -\operatorname{Im}(a_0 b_l^* \mp a_n b_t^*) \qquad R_{TL}(t) = -\operatorname{Im}(a_0 b_t^* \pm a_n b_l^*)$$

$$R_{TL'} = \operatorname{Im}(a_l b_l^* + a_t b_t^*) \qquad R_{TL'}(n) = \pm\operatorname{Re}(a_t b_l^* - a_l b_t^*)$$

$$R_{TL'}(l) = \operatorname{Re}(a_0 b_l^* \mp a_n b_t^*) \qquad R_{TL'}(t) = \operatorname{Re}(a_0 b_t^* \pm a_n b_l^*).$$

The signs in these formulae correspond to recoil polarization (upper sign) and target polarization (lower sign), respectively. The transition from system 1 to system 2 is obtained by exchanging $(t, n, l) \rightarrow (1, 2, 3)$. The coefficients a_i and b_i are combinations of the CGLN amplitudes of equation (8) as defined in table A1.

We note that the non-spin-flip part of the current (a_0) and the normal component (a_n) remain unaffected by the transition from system 1 to system 2, while the components in the reaction plane are related by a rotation with angle $(\pi - \Theta)$. (Note that the same symmetries apply for the response functions.)

References

Adamovitch M I 1976 *Proc. P N Lebedev Phys. Inst.* **71** 119
Adkins G S, Nappi C R and Witten E 1983 *Nucl. Phys.* B **228** 552
Adler S L and Dashen R F 1968 *Current Algebras and Applications to Particle Physics* (New York: Benjamin)
Adler S L and Dothan Y 1966 *Phys. Rev.* **151** 1267
Adler S L and Gilman F 1966 *Phys. Rev.* **152** 1460
Adler S L 1970 *Lectures on Elementary Particles and Quantum Field Theory* (Cambridge: Cambridge University Press)
Aguilar-Benitez M *et al* (Particle Data Group) 1990 *Phys. Lett.* **239B** 1
Amaldi E, Fubini S and Furlan G 1979 *Pion Electroproduction* (Springer Tracts in Modern Physics **83**) (Berlin: Springer) p1
Amaldi E *et al* 1970 *Nuovo Cimento* A **65** 377
Amendolia S R *et al* 1984 *Phys. Lett.* **146B** 116
Arndt R A, Workman R L, Li Z and Roper D 1990 *Phys. Rev.* C **42** 1853
Bagheri A *et al* 1988 *Phys. Rev.* C **38** 875
Bardin G, Duclos J, Magnon A, Michel B and Montret J C 1977 *Nucl. Phys.* B **120** 45
Barker I S, Donnachie A and Storrow J K 1975 *Nucl. Phys.* B **95** 347

Beck R 1989 *Thesis* University of Mainz
Beck R *et al* 1990 *Phys. Rev. Lett.* **65** 1841
Berends F A, Donnachie A and Weaver D L 1967 *Nucl. Phys.* B **4** 1
Berends F A and Weaver D L 1971 *Nucl. Phys.* B **30** 575
Berends F A and Donnachie A 1975 *Nucl. Phys.* B **84** 342
Bergstrom J C 1991 *Phys. Rev.* C **44** 1768 and private communication
Bernard V, Kaiser N, Gasser J and Meißner U-G 1991 *Phys. Lett.* **268B** 291
Bernstein A M and Holstein B R 1991 *Comment. Nucl. Part. Phys.* **44** 1768 and private communication
Bjorken J D and Drell S D 1964 *Relativistic Quantum Mechanics* (New York: McGraw-Hill) **20** 197
Blankleider B 1991 private communication
Botterill D R *et al* 1976 *Nucl. Phys.* B **116** 65
Brauel P *et al* 1974 *Phys. Lett.* B **50** 507
Breuker H *et al* 1978 *Nucl. Phys.* B **146** 285
Brodsky S J and Chertok B T 1976 *Phys. Rev. Lett.* **37** 269
Brown G E and Rho M 1979 *Phys. Lett.* **82B** 177
Burkert V 1986 *Report of the 1985 Summer Study Group* 5.1 (Research Program at CEBAF)
Cao Z J and Kisslinger L S 1990 *Phys. Rev. Lett.* **64** 1007
Chew G F, Goldberger M L, Low F E and Nambu Y 1957 *Phys. Rev.* **106** 1345
Chodos A, Jaffe R L, Thorn C B and Weisskopf V 1974 *Phys. Rev.* D **9** 3471
Chodos A and Thorn C B 1975 *Phys. Rev.* D **12** 2733
Coon S A and Scadron M D 1990 *Phys. Rev.* C **42** 2256
Copley L A, Karl G and Obryk E 1969 *Nucl. Phys.* B **13** 303
Crawford R L and Morton W T 1983 *Nucl. Phys.* B **211** 1
de Baenst P 1970 *Nucl. Phys.* B **24** 633
Donnachie A and Shaw G 1978 *Electromagnetic Interactions of Hadrons* (New York: Plenum)
Donnelly T W and Raskin A S 1986 *Ann. Phys., NY* **169** 247
Drechsel D and Giannini M M 1989 *Rep. Prog. Phys.* **52** 1083
Drechsel D and Tiator L 1984 *Phys. Lett.* **148B** 413
Drechsel D and Weber H J 1990 *Phys. Rev. Lett.* **65** 2078
Eckart G and Schwesinger B 1986 *Nucl. Phys.* A **458** 620
Ericson T and Weise W 1988 *Pions and Nuclei* (Oxford: Clarendon)
Foster F and Hughes G 1983 *Rep. Prog. Phys.* **46** 1445
Fubini S, Furlan G and Rossetti C 1965 *Nuovo Cimento* **40** 1171
Furlan G, Paver N and Verzegnassi C 1972 (Springer Tracts in Modern Physics **62**) (Berlin: Springer)
    p 118
—— 1974 *Nuovo Cimento* **20** 118, 295
Gasser J and Leutwyler H 1982 *Phys. Rep.* **87** 1
Gell-Mann M and Goldberger M L 1954 *Phys. Rev.* **96** 1433
Gell-Mann M, Oakes R J and Renner B 1968 *Phys. Rev.* **175** 2195
Goldberger M L and Treiman S B 1958 *Phys. Rev.* **111** 354
Gross F 1986 *Report of the 1985 Summer Study Group* (Research Program at CEBAF)
Holstein B R 1990 *Phys. Lett.* **244B** 83
Holzwarth G and Schwesinger B 1986 *Rep. Prog. Phys.* **49** 825
Hoodbhoy P 1986 *Phys. Lett.* **173B** 111
Isgur N and Karl G 1978 *Phys. Rev.* D **18** 4187
Kälbermann G and Eisenberg J M 1983 *Phys. Rev.* D **28** 71
Kamal A N 1991 *Int. J. Mod. Phys.* A **6** 263
Kemmer N 1938 *Proc. Camb. Phil. Soc.* **34** 354
Konen W and Drechsel D 1991a *J. Phys. G: Nucl. Part. Phys.* **17** 205
—— 1991b *Nucl. Phys.* A **529** 598
Konen W and Weber H J 1990 *Phys. Rev.* D **41** 2201
Koniuk R and Isgur N 1980 *Phys. Rev.* D **21** 1868
Kroll N M and Ruderman M A 1954 *Phys. Rev.* **93** 233
Laget J M 1981 *Phys. Rep.* **69** 1
Lattes C M G, Muirhead H, Occhialini G P S and Powell C F 1947 *Nature* **159** 694
Lee Ch, Yang S N and Lee T-S H 1991 *J. Phys. G: Nucl. Part. Phys,* **17** L131
Lee T-S H and Pearce B C 1991 *Nucl. Phys* A **530** 532
Lehmann H, Symanzik K and Zimmermann W 1955 *Nuovo Cimento* **1** 205
Lepage G P and Brodsky S J 1980 *Phys. Rev.* D **22** 2157

Low F E 1954 *Phys. Rev.* **96** 1428

Lourie R W 1990a *Nucl. Phys.* A **509** 653

——— 1990b *Preprint* UVa-INPP 90–2

Mazzucato E *et al* 1986 *Phys. Rev. Lett.* **57** 3144

Menze D, Pfeil W and Wilcke R 1977 *ZAED Compilation of Pion Photoproduction Data* (University of Bonn)

Moorhouse R G 1978 ed A Donnachie and G. Shaw *Electro-magnetic Interactions of Hadrons* (New York: Plenum)

Namyslowski J M 1984 *Progr. Part. Nucl. Phys.* **14** 49

Nath L M and Singh S K 1989 *Phys. Rev.* C **39** 1207

Naus H W L, Koch J H and Friar J L 1990 *Phys. Rev.* D **41** 2852

Nozawa S, Blankleider B and Lee T-S H 1990 *Phys. Rev.* C **41** 213

Olsson M G and Osypowski E T 1975 *Nucl. Phys.* B **87** 399

Panofsky W K H, Steinberger J N and Steller J 1950 *Phys. Rev.* **78** 802

Peccei R D 1969 *Phys. Rev.* **181** 1902

Pfeil X and Schwela Y 1972 *Nucl. Phys.* B **45** 379

Raskin A S and Donnelly T W 1989 *Ann. Phys., NY* **191** 78

Schäfer T and Weise W 1990 *Phys. Lett.* **250B** 6

——— 1991 *Nucl. Phys.* A **531** 520

Scherer S and Drechsel D 1991 *Nucl. Phys.* A **526** 733

Scherer S, Drechsel D and Tiator L 1987 *Phys. Lett.* **193B** 1

Schnitzer H J 1985 *Nucl. Phys.* B **261** 546

Schwesinger B, Weigel H, Holzwarth G and Hayashi A 1989 *Phys. Rep.* **173** 173

Simon G G *et al* 1981 *Nucl. Phys.* A **364** 285

Skyrme T H R 1961 *Proc. R. Soc.* A **260** 127

Thomas A W 1984 *Advances in Nuclear Physics* vol 13 ed J W Negele and E Vogt (New York: Plenum) pp 1–137

't Hooft G 1974 *Nucl. Phys.* B **72** 461

Tiator L and Drechsel D 1990 *Nucl. Phys.* A **508** 541c

Tomozawa Y 1966 *Nuovo Cimento* A **46** 707

Walker R L 1969 *Phys. Rev.* **182** 1729

Watson K M 1954 *Phys. Rev.* **95** 228

Weinberg S 1966 *Phys. Rev. Lett.* **17** 616

——— 1967 *Phys. Rev. Lett.* **18** 188

Weisberger W I 1967 ed M Chrétien and S S Schweber *Elementary Particle Physics and Scattering Theory* vol 1

Witten E 1979 *Nucl. Phys.* B **160** 57

Yang S N 1989 *Phys. Rev.* C **40** 1810

Yukawa H 1935 *Proc. Phys. Math. Soc. Japan* **17** 48